Journal of Water Process Engineering 50 (2022) 103301

Contents lists available at ScienceDirect

Journal of Water Process Engineering

journal homepage: www.elsevier.com/locate/jwpe

Advances in photocatalytic reduction of hexavalent chromium: From fundamental concepts to materials design and technology challenges

Ridha Djellabi [a,*], Peidong Su [b], Ehiaghe Agbovhimen Elimian [c,d,e], Valeriia Poliukhova [f], Sana Nouacer [g], Islam A. Abdelhafeez [h], Nesrine Abderrahim [i], Dominic Aboagye [a], Vaibhav Vilas Andhalkar [a], Walid Nabgan [a,k], Sami Rtimi [j], Sandra Contreras [a,*]

[a] Department of Chemical Engineering, Universitat Rovira i Virgili, 43007 Tarragona, Spain
[b] School of Chemical & Environmental Engineering, China University of Mining & Technology (Beijing), Beijing 100083, China
[c] Department of Chemical and Environmental Engineering, Faculty of Science and Engineering, University of Nottingham Ningbo China, Ningbo 315100, China
[d] Key Laboratory of Urban Pollutant Conversion, & CAS Center for Excellence in Regional Atmospheric Environment, Institute of Urban Environment, Chinese Academy of Sciences, 361021 Xiamen, China
[e] Department of Plant Biology and Biotechnology, University of Benin, Nigeria
[f] Materials Architecturing Research Center, Korea Institute of Science & Technology, 5 Hwarang-ro 14-gil, Seongbuk-gu, Seoul 02792, Republic of Korea
[g] École Nationale Supérieure des Mines et Métallurgie, ENSMM, Ex CEFOS Chaiba BP 233 RP Annaba, W129 Sidi Amar, Algeria
[h] Soils, Water and Environment Research Institute, Agricultural Research Center, Giza 12112, Egypt
[i] National Engineering School of Gabes (ENIG), RL Processes, Energetic, Environment and Electric Systems (PEESE), University of Gabes, 6072 Gabes, Tunisia
[j] Global Institute for Water, Environment, and Health (GIWEH), 1201 Geneva, Switzerland
[k] Department of Chemical and Environmental Engineering, Malaysia Japan International Institute of Technology, Universiti Teknologi Malaysia, Jalan Sultan Yahya Petra, Kuala Lumpur 54100, Malaysia

ARTICLE INFO

Keywords:
Cr(VI) photoreduction
Photocatalysis
Simultaneous removal
Heterojunction semiconductors
Metal-organic frameworks
Conjugated polymers

ABSTRACT

Toxic Cr(VI) polluted wastewater is worldwide recognized because of the wide application of chromium substances in various industrial sectors. Sustainable water pollution approaches are on demand now more than ever. In terms of Cr(VI), many homogenous and heterogenous techniques are applying to intensify its removal form water. Photocatalytic reduction of Cr(VI) has been suggested widely by the scientific community over the last two decades. This report addresses the current research state of the photocatalytic Cr(VI) reduction by addressing the most advances in terms of materials design and mechanistic pathways depending on the working conditions. The photocatalytic activity of different classes of materials such as single or heterojunction semiconductors, hybridization of photocatalyst nanoparticles (NPs) with sorbing materials, i.e., carbonaceous materials, metal-organic frameworks (MOFs), and conjugated polymers, is discussed in depth. The photodeposition of photo-produced Cr(III) on the surface of photocatalysts, and approaches to boost its desorption was addressed as well. The review discusses also the simultaneous photocatalytic reduction of Cr(VI) and oxidation of organic pollutants. A critical analysis of the current state and how to transfer substantial fundamental research to present world application was given by addressing the pros and cons of photocatalytic technology for Cr(VI) reduction compared to existing technologies. Positive research suggestions were provided to enhance the ability of photocatalytic technology for possible use, even for the purification of small volumes of industrial wastewater.

1. Introduction

Since the Industrial Revolution, chromium (Cr), widely available in the earth's crust, has been massively exploited in the industrial sector, such as textile dyes and mordants, alloying, pigments, tanning, refractory bricks, anti-corrosion materials, ceramic glazers, and pressure-treated lumber. Cr naturally exists in rocks, volcanic dust, and soil as chromite ore ($FeCr_2O_4$) or forms complexes with other metals such as bentorite $Ca_6(Cr, Al)_2(SO_4)_3$, tarapacaite (K_2CrO_4), and crocoite ($PbCrO_4$) [1]. The most stable forms of Cr are the metallic form Cr(0), hexavalent Cr(VI), and trivalent Cr(III). Cr(VI) is considered the most toxic form of chromium due to its high solubility under all pH

* Corresponding authors.
E-mail addresses: ridha.djellabi@yahoo.com (R. Djellabi), wnabgan@gmail.com (W. Nabgan), sandra.contreras@urv.cat (S. Contreras).

https://doi.org/10.1016/j.jwpe.2022.103301
Received 29 August 2022; Received in revised form 23 October 2022; Accepted 31 October 2022
Available online 8 November 2022

conditions, highly oxidative nature, large mobility in the environment, and fast penetration across living organisms' membranes. In contrast, Cr (III) represents less toxicity due to its lower mobility and relative insolubility in water [2]. In the United States and Canada, the average Cr (VI) concentrations in drinking water range between 0.2 and 2 μg/L, and the maximum limit of Cr concentration in water should be 50 μg/L. Exposure to high Cr(VI) concentration in the environment may occur naturally by weathering Cr-containing rocks or deliberately from industrial effluents, which causes severe environmental problems and threatens living organisms [3]. According to the World Health Organization, Cr(VI) is carcinogenic [4]. Besides, prolonged Cr(VI) exposure may cause teratogenicity and mutation [5,6]. The removal of Cr(VI) from water bodies is essential to preserve the ecosystem's quality and human health. Conventional techniques have been widely reported for the removal of Cr(VI) from wastewater, including adsorption [7], chemical precipitation, membrane filtration [8], ion exchange [9], reverse osmosis [10], electrocoagulation [11], electrodialysis [12], and biological reduction [13,14]. Photocatalytic technology has received tremendous attention from the scientific community over the last three decades for water remediation [15–18]. In terms of sustainability, the possible use of solar energy is an ideal and sustainable resource for environmental decontamination of organic, inorganic, microbes, and heavy metals due to its renewable, abundant, clean, and low-cost features [19–21].

The photocatalysis process depends on the photon absorption and excitation of electrons from the valence band (VB) to the conductive band (CB), and the positive holes are left in the valence band, enhancing the catalyst surface redox reaction [22]. Photocatalysis is a process that can be used to oxidize organic/inorganic pollutants or reduce heavy metals due to the redox system generated on the CB and VB of a photocatalyst. Over more than two decades, the photocatalytic reduction of Cr(VI) has received much attention from the scientific community by emphasizing several research axes (Fig. 1), including understanding the concept of electrons transfer to Cr(VI) or indirect reduction via the generation of reductive species, the role of hole scavenger to liberate electrons and react with positive holes and reactive oxygen species (ROSs), the effect of pH on Cr(VI) speciation and the edges of CB and VB of semiconductor, and the behaviour of produced Cr(III) species (deposition or desorption). Over the last decade, more studies have been reported on the design of novel classes of photocatalytic materials for enhanced photocatalytic reduction through common approaches,

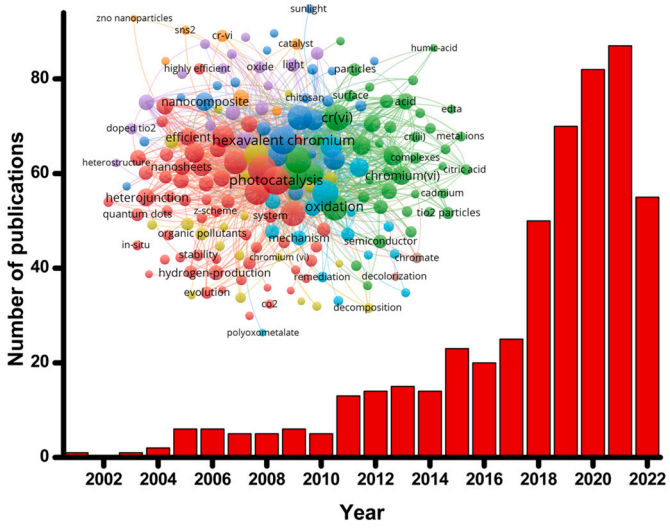

Fig. 1. Number of publications per year on photocatalytic Cr(VI) reduction. The map, obtained by VOSviewer, shows the hopttest topics in terms of Cr(VI) photoreduction over more than two decades. Data were collected from Web of science, keyword: Photocatalytic Cr(VI) reduction, from 2000 to August-2022.

including increased light absorption, charge separation, adsorption ability, or other purposes, i.e., enhancing the fixation of Cr(VI) by ion-exchange reaction, boost the desorption of produced Cr(III). Different classes of photocatalysts have been used to photocatalytically reduce Cr (VI) into Cr(III) such as single semiconductors, i.e., TiO_2 [23], g-C_3N_4 [24], ZnO [25], WO_3 [26], Ag_3PO_4 [27], and semiconductor heterojunctions, i.e., Ag_3PO_4/Fe_3O_4 [28], $CuAl_2O_4/TiO_2$ [29], Bi_2O_3/BiOI [30], $ZnIn_2S_4/SnS_2$ 3D [31]…etc., semiconductor coated adsorptive materials such as carbon [32] and clays [33], and polymer based photocatalysts [34,35].

The aim of this review is to summarize the advances done on Cr(VI) reduction, and addresses the hottest topics and discussion. Cr(VI) can be photocatalytically reduced via two ways, namely one step three-electron transfer, and three steps of single-electron transfer. The effect of operating parameters and the presence of hole scavenger molecule can affect the reduction process, i.e., electrons can be better accumulated on the conduction band of the photocatalyst which in turn boosts the one step transfer reduction process. The design of smart materials to solve some general issues in photocatalysis, and particularly Cr(VI) photoreduction is addressed in details. This review gives the reader more clarity about the application of photocatalysis for Cr(VI) reduction from fundamental research to technological advances.

2. Principles of photocatalytic reduction of Cr(VI)

The principle of Cr(VI) photoreduction has been addressed, and many mechanistic pathways were suggested. In general, the reduction of Cr(VI) by photocatalytic means occurs by photocatalytic photogenerated electrons on the CB of the semiconductor. To make this reaction happen, the CB edge needs to be more negative than the redox potential of Cr(VI)/Cr(III). Cr(VI) cannot be reduced to metallic state (Cr (0)) because Cr(III)/Cr(0) has high negative redox potential. In terms of Cr(VI) reduction, electrons move directly to adsorbed Cr(VI) or even at the boundary of the photocatalyst surface. The transfer of electrons from the CB to Cr(VI) can be rooted in two ways [36,37]. In one way, Cr(VI) can be reduced directly to Cr(III) by one step transfer of three-electrons from the conduction band of photocatalyst. In another way, Cr(VI) is reduced through single electron transfer, producing Cr(V) and Cr(IV) as intermediates [38–40]. The photoreduction of Cr(VI) consumes protons; therefore, the acidic medium is more favourable. Since the surface of photocatalyst can produce ROS and oxidative positive holes, unwanted reactions in terms of oxidation of produced Cr(III) might take place to reverse the reaction (Eq. 3). To equilibrate the photoreduction of Cr(VI), hole scavenger molecules can be added to the medium, principally to react with oxidative species, including ROSs and positive holes [41]. The more the interaction with holes and ROS, the more efficient Cr(VI) reduction will be. The efficiency of photocatalytic reduction of Cr(VI) depends significantly on the nature of used hole scavenger molecule [42,43]. The scavenging of holes allows an enhanced separation of electrons in the CB, which may result in one three-electron reduction transfer mechanism (eq. 1). While, in the absence of any hole scavenger molecules (pure water), the photoreduction of Cr(VI) is a very slow reaction following the four-electron transfer process (eq. 2) due to the rapid recombination of e^-/h^+ charges [44,45].

$$Cr_2O_7^{2-} + 14H^+ + 6e^- \rightarrow 2Cr^{3+} + 7H_2O \quad (1)$$

$$Cr(VI) \xrightarrow{e^-} Cr(V) \xrightarrow{e^-} Cr(IV) \xrightarrow{e^-} Cr(III) \quad (2)$$

$$Cr(III) + ROSs \rightarrow Cr(VI) \quad (3)$$

It was reported that one mole of $^{-}\bullet O_2$ photoproduced simultaneously on the CB can reduce Cr(VI) to Cr(V) [46,47]. Some studies reported that the pumping of oxygen into the reaction medium would enhance the reduction of Cr(VI) because of the enhanced formation of $^{-}\bullet O_2$ species [48]. In addition, reducing chemical species can be produced from the oxidation of hole scavenger molecules, i.e., $CO_2^{\bullet -}$ ($E_0(CO_2/CO_2^{\bullet -}) \approx -$

2.0 V, which are able to participate indirectly in the reduction of Cr(VI) [43]. The mechanistic photocatalytic reduction of Cr(VI) with and without the presence of a hole scavenger is schematized in Fig. 2(a, b). Since the addition of chemicals into wastewaters during the purification is considered a less sustainable process, many studies were devoted to the simultaneous oxidation of photoorganic pollutants and photoreduction of Cr(VI).

The pH of the medium is a predominant factor in controlling the photocatalytic reduction since the presence of protons is required. On top of that, there are other reasons behind the enhanced reduction in acidic medium. The transfer of electrons from the CB to Cr(VI) species occurs mostly after the electrostatic interaction, as shown in Fig. 2,c (pathway 1). On the contrary, it is less possible that photogenerated electrons can reduce Cr(VI) species in the bulk solution (pathway 2). In this regard, as shown in Fig. 2,d, strong electrostatic interactions can take place in an acidic medium while decreasing at higher pH values. Many studies showed that the photoreduction at pH higher than 7 is almost negligible [42,45]. Cr(VI) exists in different forms as oxy-anions depending on the pH of the medium (Fig. 3). At pH close to neutral and low Cr(VI) concentration, chromate CrO_4^{-2} is expected to be predominant, and protonation of CrO_4^{-2} occurs to form $HCrO_4^-$. At a very low pH value, further protonation occurs to form H_2CrO_4 species. These Cr(VI) species exhibit different redox potentials at different pH values (Fig. 2, e). In fact, the redox potential of Cr(VI)/Cr(III) anodically shifts by -0.14 V pH^{-1}, which in turn improves the driving force between the CB and the Cr(VI)/Cr(III) at lower pH values [49]. In addition, the pH can shift both the CB and VB of the photocatalyst. For example, TiO_2 (anatase), the CB shifts from -0.1 V to -0.45 V as pH varies from 1 to 7 [43]. It is worth mentioning that the concentration of Cr(VI) or the coexisted ions might affect the redox potential and edges of CB and VB.

Another issue that should be investigated is the behaviour of produced Cr(III) after the reduction of Cr(VI). Two possibilities can take place, surface deposition of Cr(III) and Cr(III) release in the solution. The formation of $Cr(OH)_3$ can occur even at acidic and alkaline solutions

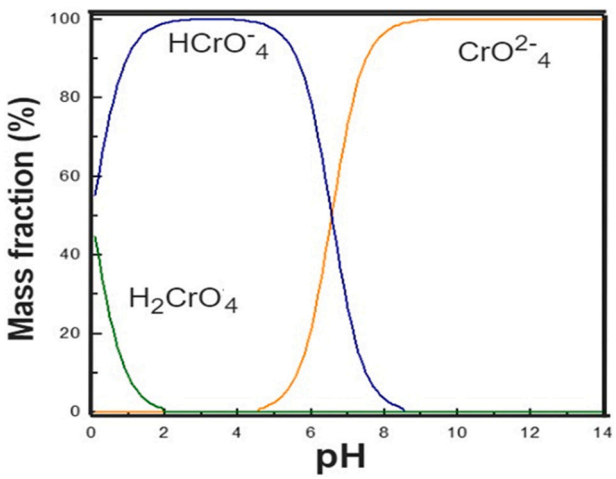

Fig. 3. Speciation of Cr(VI) as a function of pH and concentration.

[50,51], while at very acidic pH < 1, the formation of $Cr(OH)_3$ is less expected [52]. The deposition of Cr(III) species is a serious issue during the photocatalytic reduction of Cr(VI) as it blocks the surface and prevents the penetration of light and the access of Cr(VI) to the photocatalyst surface. In addition, Cr(III) deposited on the surface can play a role in promoting the recombination of e^-/h^+ charges, especially if the surface area of the photocatalyst is low [53]. Djellabi et al. [23] have estimated the amount of photo-deposited Cr(III) on the surface of TiO_2. As shown in Fig. 4, the colour of TiO_2 turned green because of the deposition of Cr(III) species. It was found that around 40 % of Cr(III) was deposited, and the rest was released in the solution. The authors used sequential extraction to remove Cr(III) from the TiO_2 surface. Through sequential extraction (three times), the total extraction rates were found to be 90.1 and 42.6 % for citric acid and EDTA as extracting agents,

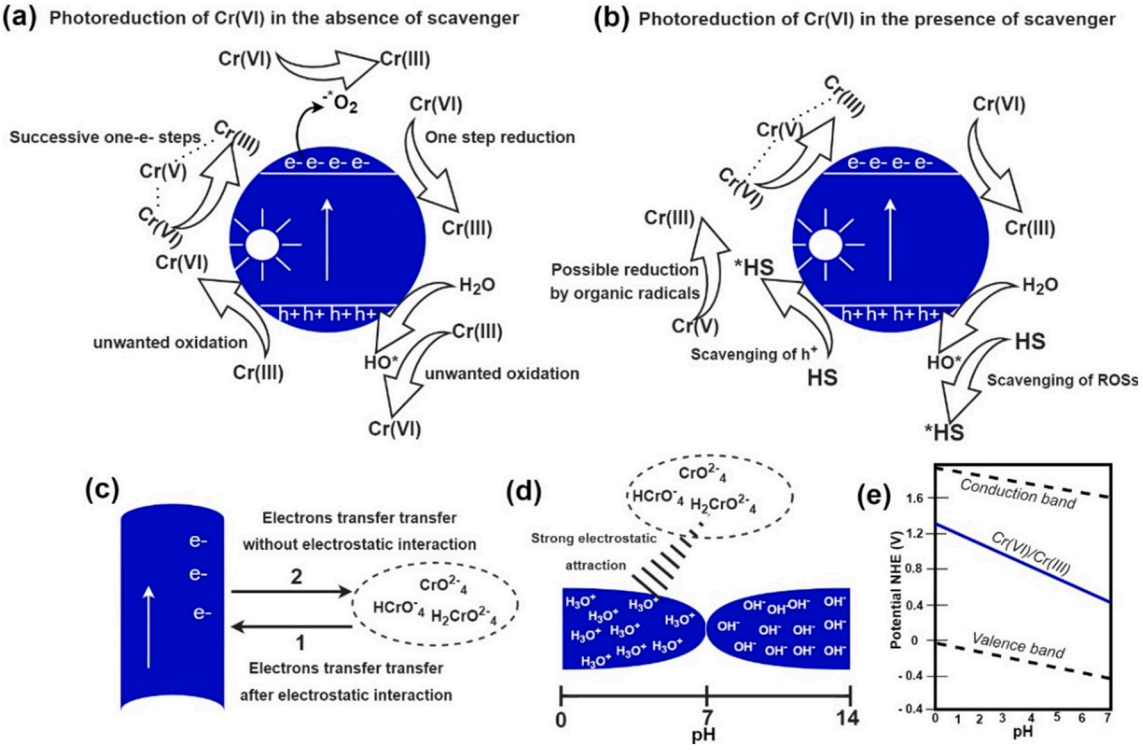

Fig. 2. (a) and (b): photocatalytic reduction of Cr(VI) with and without hole scavenger (HS) molecule. (c): Possible pathways of electrons transfer from the conduction band to Cr(VI) species. (d): Electrostatic interactions of Cr(VI) species as a function of pH of a solution. (e): effect of pH on the conduction/valence bands of TiO_2 and redox potential of Cr(VI)/Cr(III) (obtained from the Nernst equation).

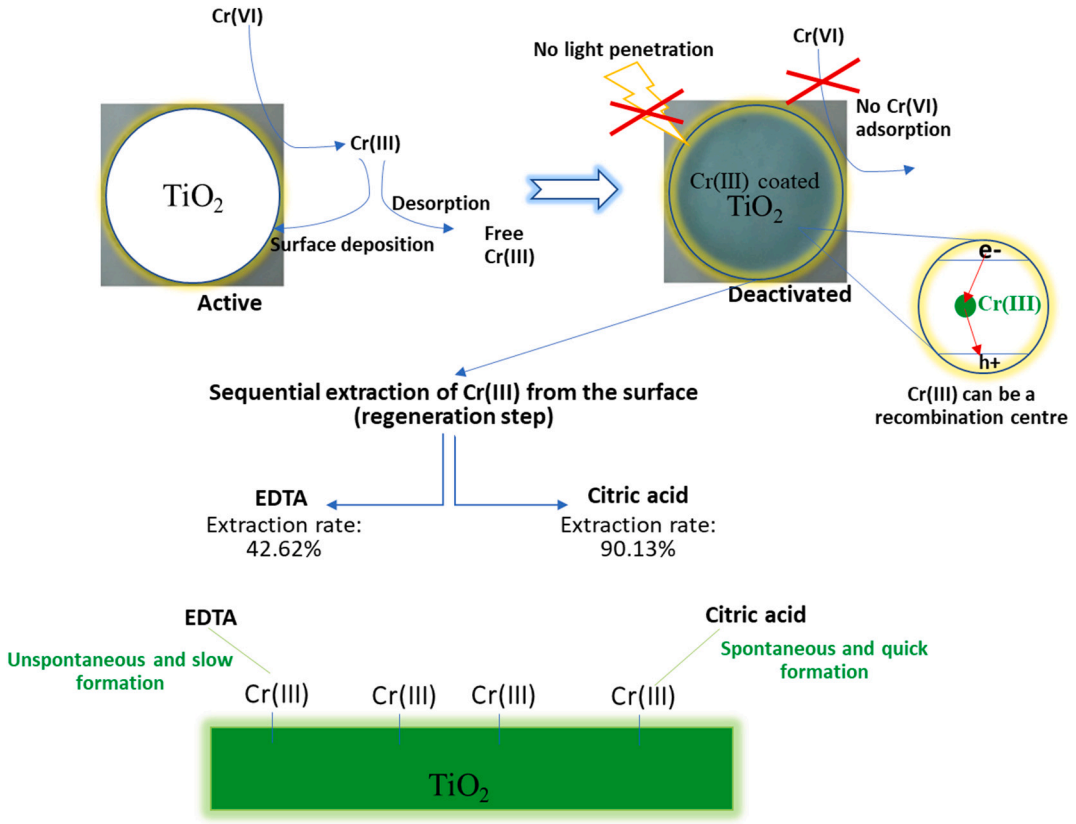

Fig. 4. Deposition of produced Cr(III) on TiO_2 surface and TiO_2 regeneration by sequential extraction (produced based on the results of ref. [23]).

respectively. The extraction mechanism is based on the formation of complexes between the extracting agent and Cr(III) deposited species, and the better the complexation, the better the release of the Cr(III)-agent from the surface. It was reported that citric acid could form spontaneously and quickly mononuclear anion $[Cr(C_6H_4O_7)(C_6H_5O_7)]^{4-}$ which is more favourable compared to Cr(III)-EDTA, which needs boiling. The modification of the surface of the photocatalyst could solve the problem of fast deactivation of TiO_2 by Cr(III) deposition. A simple coating of TiO_2 by hydroxyl groups improves the fixation of Cr (VI), as well as the desorption of produced Cr(III) from the surface of the photocatalyst [54]. The photocatalytic reduction of Cr(VI), similar to other pollutants, depends also on several operating parameters such as the initial concentration of Cr(VI), the dosage of photocatalyst, intensity and type of light irradiation, and the presence of interfering ions [42,55–57].

3. Advances in materials design for Cr(VI) photoreduction

3.1. Inorganic semiconductor

Semiconductors have different performances towards the photoreduction of Cr(VI). In fact, the semiconductor with more negative CB and a high yield of separated electrons would perform better. In addition, a semiconductor with lower oxidative power is more suitable for the reduction of Cr(VI) into Cr(III) as unwanted oxidation of Cr(III) is less pronounced. The surface interactions in terms of electrostatic attraction can boost photocatalytic reduction. Therefore, a lot of studies proved that the modification of the charge of photocatalyst surface to more positive might enhance the interaction with Cr(VI), resulting in better photoreduction. Djellabi et al. [26] have tested several photocatalytic semiconductors with different band gaps and conduction band edges, Fig. 5a, and it was found that Fe_2O_3 and g-C_3N_4 were the most effective one (Fig. 5b). It was estimated that Fe_2O_3 has the best Cr(VI) performance because it combines the photocatalytic production of electrons and direct Cr(VI) reduction by iron species. However, in terms of pure photocatalytic reduction, g-C_3N_4 was the best due to its high conduction band compared to others. Photocatalytic heterojunction systems were widely reported for enhanced photocatalytic reduction of Cr(VI) due to the promoted charge carriers transfer in different heterojunction schemes such as ZnO/ZnS [58], Cu_2O/Bi_5O_7I [59], Bi_5O_7I/ZnAlBi-CLDHs [60], Ag_3PO_4/g-C_3N_4 [46], $Bi_2WO_6/Bi_2S_3/MoS_2$ [61], BiO_{2-x}/BiOCl [62], $ZnIn_2S_4$/g-C_3N_4 [63], AgI/TiO_2 [64], TaON/Bi_2MoO_6 [65], etc. An example of a heterojunction system for Cr(VI) reduction is shown in Fig. 5c; a *Z*-scheme $AgIn_5S_8/SnS_2$ ($AgIn_5S_8$ abbreviated as AIS) was designed for enhanced reduction of Cr(VI) [66]. The composite of ZnO/ZnS, also based on a Z-scheme, removed 100 % of Cr(VI) within 60 min at 50 ppm [58]. It was found that bare AIS and SnS_2 showed only 9.6 and 45.9 % towards Cr(VI) reduction within 100 min at 10 ppm, respectively. At the same time, AIS/SnS_2 can totally reduce all Cr(VI) species in the solution within 20 min. Cr(III) deposition on the surface of photocatalysts could be an issue during the real-world application, as the photocatalyst could be deactivated and no further light absorption can take place. The deposited Cr(III) could be removed by extraction [23], but it is costly and a long step process. Zhang et al. modified TiO_2 by carbon dots originally to improve the separation of electrons for enhanced Cr(VI), and to enhance the selective adsorption of Cr(VI) species because of positively charged carbon dots-TiO_2 [36]. On the other hand, a fast desorption of produced Cr(III) species was found, which allows recyclability (Fig. 5d).

3.2. Combination of photocatalysis with adsorbent-based materials

One of the approaches to enhance the photocatalytic reduction of Cr (VI) is the combination of semiconductor nanoparticles with adsorbing materials. In general, the hybridization of photoactive nanoparticles with adsorptive materials has been suggested as an excellent approach

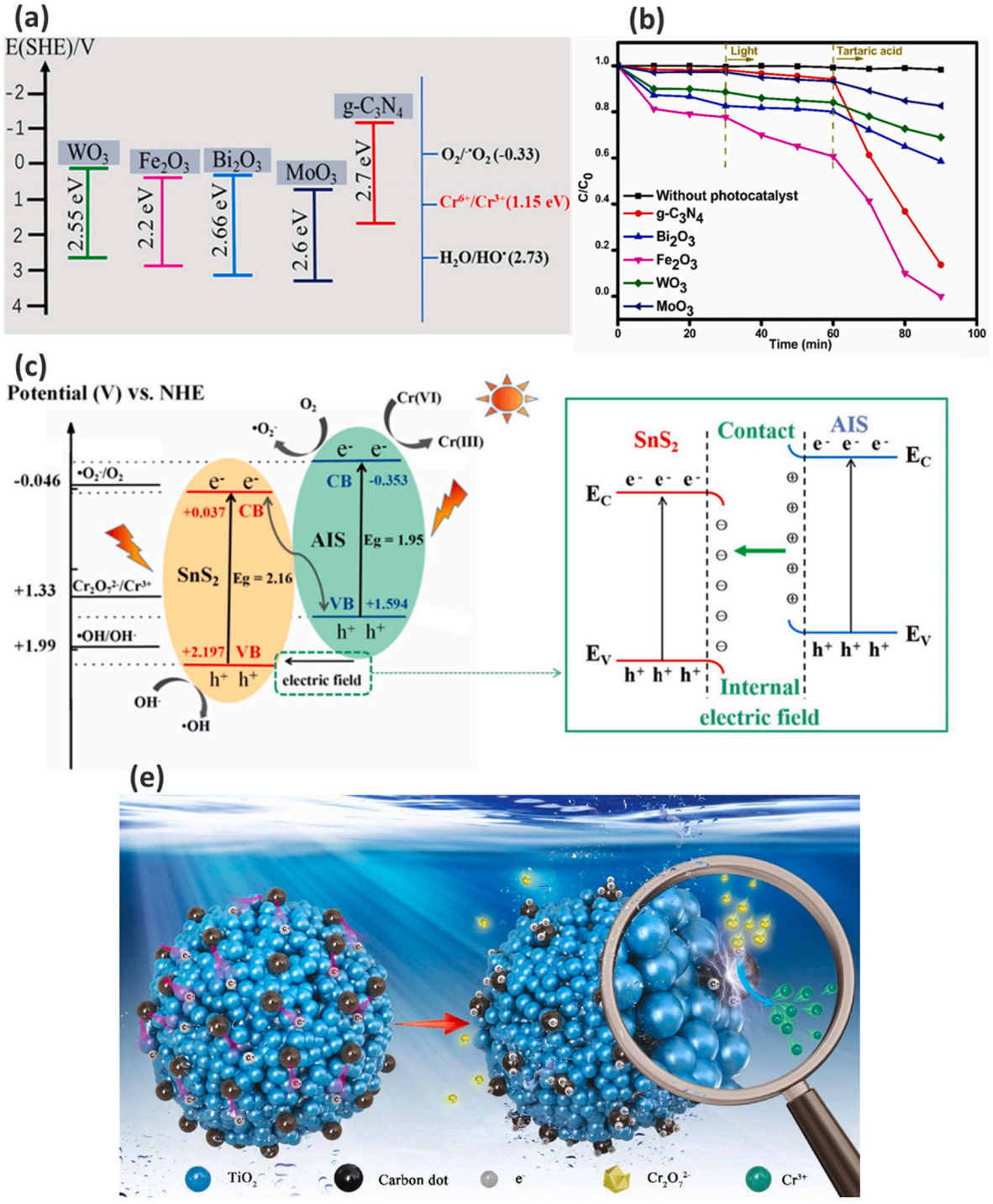

Fig. 5. (a) and (b): Redox potential of different photocatalysts, and their photocatalytic behaviour towards Cr(VI) reduction under visible light, (a) and (b) reproduced with permission from [26]. (c): Z-scheme AIS/SnS_2 heterojunction towards the photocatalytic reduction of Cr(VI), reproduced with permission from [66]. (d): carbon dots modified TiO_2 for enhanced adsorption/reduction of Cr(VI) and easy desorption of produced Cr(III), reproduced with permission from [36].

to enhance the removal of pollutants from one side and solve some technological issues from another side. Several synergistic pathways can take place on the surface of such composites, known as Adsorb and Shuttle process (Fig. 6a) [67–69]. Using naked photocatalytic nanoparticles has many drawbacks, such as the low adsorption ability and mass transfer, which limits the interaction of pollutants with photogenerated species (electrons or reactive oxidation species) since most redox reactions occur on the surface of the photocatalyst. A single photocatalyst can produce a high yield of by-products, and most of them are released into the solution. Fast deactivation of single-component photocatalysts is a common issue, which requires continuous regeneration after a certain time of use. After the treatment, the recovery of nano-sized particles from water is very hard and requires a lot of energy. The toxicity of the nanoparticles has been criticized recently in many reports [70–72]. On the other hand, the fixation of nano-sized particles on the surface of highly porous and adsorptive materials enhances the mass transfer by concentrating the pollutants species on the surface to be easily oxidized/reduced by photogenerated species. This process works continuously and cooperatively. The oxidation of pollutants on the surface also solves the problem of adsorbents' fast saturation. By-

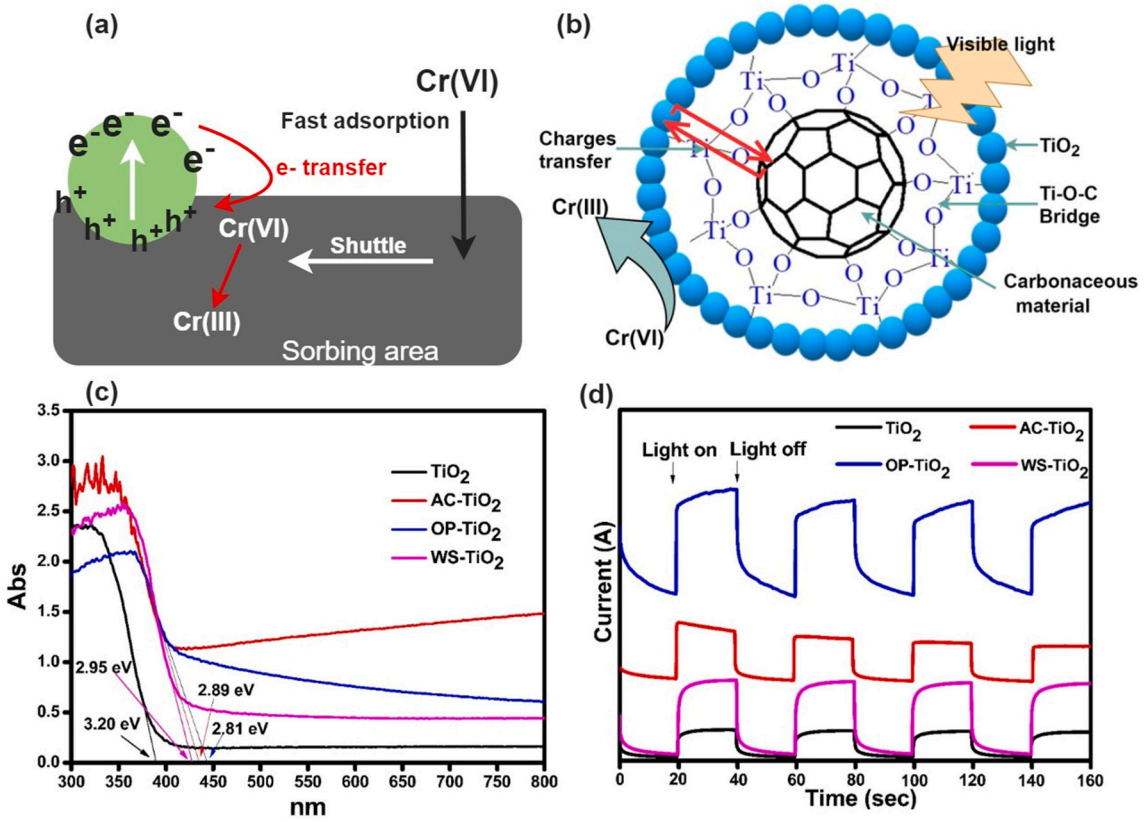

Fig. 6. (a): The principle of Adsorb & Shuttle process towards the photocatalytic reduction of Cr(VI). (b): TiO_2 hybridized carbon-based materials and mechanistic pathways for enhanced charge transfer, visible light absorption, and photoactivity. (c) and (d): narrowed band gaps and enhanced photocurrent activities in Activated carbon-TiO_2, olive pits-TiO_2, and wood shaving-TiO_2 composites compared with bare TiO_2. Reproduced with permission from [90].

products generation would be lesser as well in this composite system. In addition, the separation of particles after the treatment would be easier as compared to nano-sized photocatalysts. In terms of Cr(VI), a huge number of sorbing/photoactive composites were reported such as montmorillonite-TiO_2 [73], montmorillonite-Ag_3PO_4 [74], graphene-ZnO [75], reduced graphene-TiO_2 [76], lignocellulosic biomass-TiO_2 [77], active carbon/BiOI [78], activated carbon-$CoNiWO_4$-gCN [79], Fe_2O_3-clay [80], CdS–reduced graphene oxide [81] and so on. The hybridization of TiO_2 with carbonaceous materials leads to a fascinating enhancement in visible light absorption and charge transfer. TiO_2 hybridized with carbon materials such as activated carbon, graphite, carbon nanotubes, or fullerene showed enhanced photocatalytic activity under visible light as proved by a pool of studies [82–86]. This is because their delocalized conjugated structures allow the formation of interfacial electronic interactions and strong bonds which in turn work as a charge exchange bridge between the photocatalytic nanoparticles and carbon materials. In this regard, the carbon material can act as an electron receiver, reducing the recombination of $e-/h^+$ charges on the surface of the photocatalyst [87,88]. Carbon materials are also excellent photosensitizers to photoexcite non-visible light-based semiconductor, TiO_2, as proved by many studies [77,86,89,90]. It was reported that the hybridization of TiO_2 nanotube arrays with graphene (GO) enhanced the photochemical/photocatalytic abilities by 15 times as compared to bare TiO_2 [91,92]. The interaction between carbon material and semiconductor might decrease as well the band gap [93,94]. The synthesis method used for the preparation of photocatalytic/adsorbent composite determines the desired physical and photonic characteristics. The ultrasonic process is one of the approaches that could help to design nanomaterials with enhanced properties [95]. Djellabi et al. have hybridized TiO_2 by ultrasonic-assisted sol-gel with different supports such as activated carbon, olive pits biomass, and wood shaving biomass [77,90]. The authors claimed that, Ti-O-C bonds as bridge were formed between TiO_2 nanoparticles and biomass. In terms of activated carbon, Ti-O-C was not obvious; however, olive pits as a support showed very intense Ti-O-C bonding bridge. As shown in Fig. 6b, this bridge promotes the visible light absorption and charges transfer. Photocatalytic studies showed that these materials can reduce effectively under visible light, unlike bare TiO_2. A red shift and narrowed band gaps were also observed (Fig. 6c). In addition, the photochemical current was several times better as compared to bare TiO_2 as a result effective charge separation (Fig. 6d).

3.3. *Metal-organic frameworks (MOFs)*

Metal-organic frameworks (MOFs) are functional hybrid inorganic-organic materials that represent an attractive platform for the study of complex reactions owing to the wide variety and easily tailored structures [96,97]. MOFs are made up of metal-oxo clusters joined by organic linkers through strong chemical bonding that gives the three-dimensional (3D) porous material structural integrity. MOFs, unlike other microporous counterparts like zeolites, are responsive to external stimuli and can perform photochemical processes in response to photoexcitation of the organic linker, mimicking the behaviour of a photocatalyst. MOFs outperform typical photocatalysts specifically due to their large surface area ($>1000\ m^2g^{-1}$) and abundant active sites, and tuneable pore diameters. For instance, MOFs exhibit several advantages over traditional semiconductor-based photocatalysts, including enhanced visible light absorption and excellent electron/hole production. The efficient light harvesting may be achieved by fine-tuning the HOMO-LUMO gap of MOFs at the molecular level by rational alteration of the inorganic moiety or organic linker [98,99]. These intrusive characteristics have increased the application of MOFs in various fields

such as catalysis [100,101], separation [102,103], gas storage [104], carbon dioxide capture [105], and so on [106]. In MOFs systems, the organic linkers function as photo-harvesters that generate excited electrons upon light absorptions and undergo metal-to-ligand charge transfer (LMCT)). On this basis, the appropriate choice of inorganic metal clusters and organic linkers is important for visible light harvesting. Enormous modification strategies such as the use of MOF-ligand functionalization, encapsulation of semiconductors/photosensitizers, and coupling with other materials like transition metal, noble metals, and carbon have been explored to enhance the photoreduction of Cr(VI) under UV–visible light region [107,108]. Based on these strategies, the band gap of the pristine MOF is reduced to about 3.0 eV. For example, the coupling of ZIF-8 (a band gap of 5.1 eV) with nanoparticles such as CuPd [107] and $Cd_{0.5}Zn_{0.5}S$ [109] resulted in a lower band gap of 2.65 eV and 2.53 eV, respectively compared to the pure ZIF-8. The scientific advancement of MOF applications in photocatalytic Cr(VI) reduction has been emphasized, as listed in Table 1. To summarize the catalytic performance and reaction mechanism, representative examples of typical amine-functionalized MOFs, semiconductor/MOFs composites, noble metal/MOFs composites, and carbon/MOFs composites were selected.

As earlier stated, the application of pristine MOFs is limited because of the wide bandgap that only permits activation under UV light. The photosensitive nature of MOFs was first observed with MOF-5, which has an absorption excitation of 400 nm, making it viable to be used as a photocatalyst [110]. The addition of the amine functional group to MOF photocatalysts is a common approach used to promote the visible light response ability [111,112]. The addition of the - NH_2 group can have a major impact on O to Ti charge transfer (LMCT) to build visible light responsive NH_2-MIL-125(Ti) up to 520 nm [113,114]. MOFs based photocatalysts such as MIL-125 [115], MIL-68, NH_2–MIL-88B (Fe) [116] MIL-68(In)-NH_2 [117], UiO-66(NH_2) [118], and UiO-66-NH2(Zr/Hf) [113] have been reported to have excellent photoreduction of Cr(VI). Shi et al. [119] reported that the amine-functionalized iron(III) MOF (NH_2–MIL-88B (Fe)) was very effective for Cr(VI) photoreduction and stable in terms of recycling compared to MIL-88B (Fe) and commercial TiO_2 (P25). It was proved that the addition of amine groups was the reason behind the higher visible light response. Fe(III)-based MOF increases visible absorption. In addition, amine functionality stimulates the production of more electron-hole pairs under visible light to be transferred to Fe_3-μ_3-oxo clusters resulting to increased photocatalytic activity. The modification of the charge of MOFs surface can significantly improve the fixation and reduction of Cr(VI). Highly cationic charged Ru-UiO-dmbpy(1) linked with an excellent visible light responsive moieties ($Ru(bpy)_3$) was reported [120]. As shown in Fig. 7a, Ru-UiO-dmbpy(1) plays an important role in fixing Cr(VI) anions by ion-exchange reaction followed by reduction via photogenerated electrons. The adsorption was enhanced 8.26 times compared to bare UiO-bpy, while the photocatalytic reduction was outstandingly promoted, wherein the photocatalytic reduction rate constants were found to be (k_1) of 0.011 min^{-1} for Ru-UiO-dmbpy(1) against 0.003 min^{-1} for bare pristine UiO-bpy under visible light without the addition of hole scavenger. The fabrication of semiconducting MOF-semiconductor heterojunctions is an effective strategy to improve the photogenerated charge-separation efficiency and is crucial for promoting the photocatalytic reduction of Cr(VI). The synthesis of unique MOFs nomenclature by combining with other semiconductor materials leads to the formation of heterojunctions that capture and transfer the electrons across the interface from one material to another, resulting in efficient charge separation and improved selectivity of catalysts. The binary composite composed of $Bi_{24}O_{31}Br_{10}$@BUC-21 achieved a photocatalytic reduction of 99 % compared to BUC-21 (22 %) under visible light. The excellent performance was attributed to the enhanced electron transfer displayed by the $Bi_{24}O_{31}Br_{10}$@BUC-21 compared to bare BUC-21 MOF [121].

In addition, the controllable incorporation of noble metals into the MOFs can equally improve the absorption of light and enhance the production of separated charges. The localized surface plasmon resonance (LSPR) effect of the noble metals could further enhance the solar-

Table 1
MOF -based nanomaterials applied for Cr(VI) photoreduction.

S/N	MOF-based nanomaterial	Bandgap energy (eV)	BET specific surface area (m^2/g)	catalyst mass (mg)	wavelength (nm)	Reaction Time (min)	Removal efficiency	Ref
A. Titanium MOFs								
	NH_2- MIL-125(Ti)	2.65	1344	2.0	420	60	97	[115]
	NTU-9/NH_2-MIL-125	2.22	1267	20.0	450	90	70	[131]
	CuS/MIL-125(Ti)	–	1303	2.5	420	75	55	[132]
B. Zirconium MOFs								
	UiO-66-$(OH)_2$	2.8	561.5	5.0	420	40	80	[133]
	UiO-66(NH_2)	–	756.04	2.0	420	80	97	[118]
	UiO-66-NH_2@$ZnIn_2S_4$	2.42	–	3.0	420	30	100	[134]
	RGO-UiO-66(NH_2)	–	767	2.0	420	100	100	[130]
	Pd@UiO-66-NH_2		836.6	2.0	420	90	99	[99]
	Ag/AgCl/NH_2-UiO-66	2.83	–	25.0	420	150	74	[135]
C. Iron MOFs								
	MIL-53(Fe)	2.72	–	4.0	420	40	100	[136]
	MIL-53(Fe)/SnS	–	34.0	5.0	420	60	71.3	[137]
	g-C_3N_4/MIL-53(Fe)	2.51	18.5	2.0	420	180	100	[125]
	MIL-101(Fe)/g-C_3N_4	2.26	131.6	2.0	420	30	100	[138]
	NH_2-MIL-88B(Fe)/CD-50	1.98	29.8	2.0	420	30	95	[139]
D. Transition metals								
	MIL-68(In)–NH_2	2.82	674	4.0	420	180	97	[140]
	MWCNT/NH_2-MIL-68(In)	2.43	801	4.0	420	60	100	[141]
	Cd-MOF1	2.98	–	7.0	365	50	100	[142]
	CdS/MOA(Cr)-20	1.7	714.4	5.0	420	120	99	[143]
	Zn-MOF	2.12	–	1.5	420	30	96	[144]
	NH_2– ZIF-8	–	1025	2.0	400	180	96	[145]
	$Cd_{0.5}Zn_{0.5}S$@ZIF-8 (CZS@Z60)	2.53	174	4.0	420	10	100	[109]

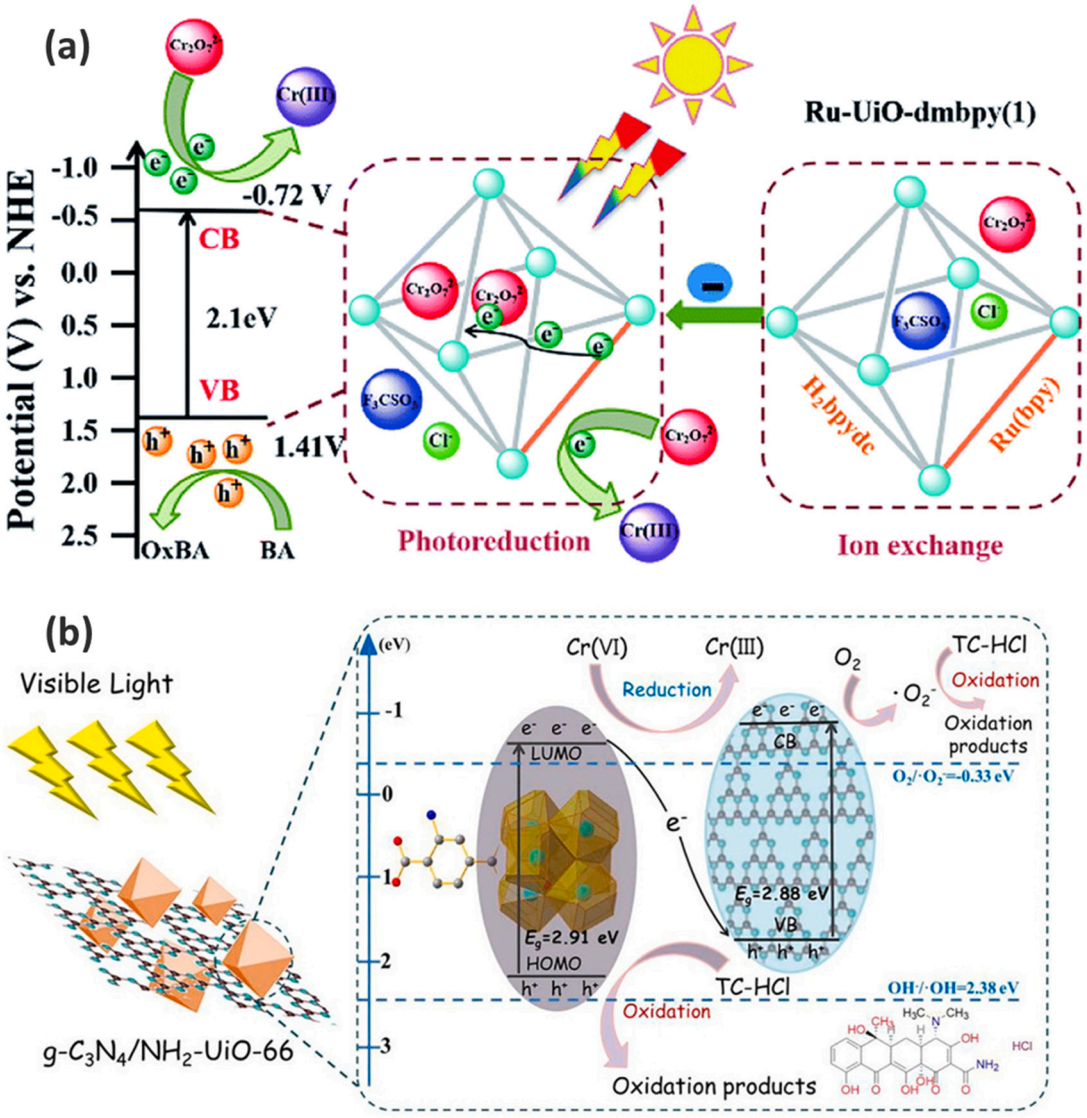

Fig. 7. (a): Ru-UiO-dmbpy(1) based MOFs for enhanced photoreduction of Cr(VI). Reproduced with permission from [120]. g-C_3N_4/NH_2-UiO-66 (Zr) heterojunction for Cr(VI) photocatalytic reduction and tetracycline hydrochloride (TC-HCl) oxidation, reproduced with permission from [129].

energy conversion efficiency of photocatalyst [122,123]. The tailorable structure and tuneable pores of MOFs-based photocatalysts permit the immobilized noble metal nanoparticles onto MOFs' framework. In system Pd@UiO-66(NH_2), Pb plays an important role in producing charges and enhancing their separation, wherein a high reduction rate was obtained compared to Pb free MOF [99].

The hybridization of MOFs with carbon materials such as carbon dots (CDs), carbon quantum dots (CQDs), graphene, and g-C_3N_4 has achieved high photoreduction. Lin and colleagues [124] synthesized MIL-53(Fe)/CQD to overcome this limitation associated with rapid charge recombination. The synthesis of MOF nanocomposites MIL-53(Fe)/CQD displayed promoted visible light response due to the n–π* and π–π* transitions in CQDs. The MIL-53(Fe)/CQD completely reduced Cr (VI) photo-catalytically during the 50 min reaction time compared to the MIL-53 (Fe), achieving a moderate reduction of 48 % because of charges transfer between Fe_3-μ_3-oxo cluster and CQD. CQD can act as a photosensitizing to promote the excitation rate of the composite.

The fabrication of MOF/g-C_3N_4 hybrid composites results in improved photocatalytic performance attributed to increased pore volume, effective charge carrier separation, reduced recombination rate of photogenerated charges, and broad solar spectrum absorption. The pristine g-C_3N_4 is associated with restacking and aggregation; however, the MOFs in MOF/g-C_3N_4 hybrids help prevent restacking and aggregation. Several g-C_3N_4/MOFs hybrids such as MIL-101(Fe)/g-C_3N_4 [125], g-C_3N_4/MIL-53(Fe) [126], g-C_3N_4/UiO-66 [127], BUC-21/g-C_3N_4 [128], g-C_3N_4/NH_2-UiO-66 (Zr) [129] have been widely reported for Cr(IV) photocatalytic reduction. An example of a g-C_3N_4/MOFs hybrid composite is shown in Fig. 7b. It showed the z-scheme of g-C_3N_4/NH_2-UiO-66 (Zr) heterojunction promotes Cr(VI) reduction and TC-HCl oxidation [129]. The combination of MOFs with reduced graphene oxide (rGO) showed an excellent synergistic effect on the fast photocatalytic reduction of Cr(VI), including enhanced light absorption, charge separation, excellent surface area, and better stability. It was reported that the incorporation of rGO into UiO-66(NH_2) improves the light absorption up to 800 nm [130]. Therefore, enhanced Cr(VI) degradation was found due to improvement in adsorption ability and longer photogenerated electrons life time. However, the optimization of rGO that is incorporated in the MOFs is important to balance among the physical, photonic, and photocatalytic characteristics.

3.4. Photoactive organic polymer

Organic polymers as photocatalysts have been used recently for the removal of a wide range of organic and inorganic pollutants from water

or air [34,35,146]. Organic conjugated polymeric photocatalysts show several advantages as compared to inorganic semiconductors, such as highly tuneable photonic and electronic characteristics, less toxic and easy-to-prepare in some cases [34,147–149]. On top of that, conjugated polymers (CPs) redox potential can be easily and precisely controlled by changing or combining with a given electron donor or electron acceptor compounds [150]. CPs that exhibit extended n → π* and π → π* transitions give result in promoted optical, longer-lived charge carriers and photocatalytic characteristics [151]. CPs can be used as a photocatalyst to reduce Cr(VI) directly or/and to enhance the photonic and physical characteristics of inorganic semiconductors for synergistic and enhanced reduction [148,152,153]. Among polymeric photocatalysts, graphitic carbon nitride (PCN) has been regarded as a promising material due to its synthesis, stability in water at different pH, thermal stability, relatively small band gap (2.7 eV), and also excellent photoactivity [154,155]. Even though PCN has moderate oxidation ability, it received a lot of attention towards the photoreduction of Cr(VI), showing better efficiency than many other bare common photocatalysts because of its negative CB [26]. Li et al. [156] edited the electron-donating ability of conjugated heptazine polymers by inserting different heteroatoms (dibenzofuran, carbazole, dibenzothiophene) for Cr(VI) under visible light. All modified heptazine polymer composites showed excellent photoreduction of Cr(VI) as compared to unmodified because of the enhancement in the electronegativity of CB and promoted charge separation. The modification of CPs by ferrocene might also promote the photocatalytic reduction of Cr(VI). Wang et al. [157] reported the synthesis of two CPs based on 4,4′-biphenyldicarboxaldehyde and 2,4,6-tris(4-aminophenyl)-1,3,5-triazine, namely ferrocene-containing CPs and ferrocene-free analogue. It was found that ferrocene-containing CP (1 g/L) is able to reduce 99 % of Cr(VI) at 25 ppm within 15 min under visible light, while ferrocene-free analogue showed a reduction rate of 99 % within 60 min. The introduction of ferrocene units into the backbones of CPs limits the recombination of charges and results in routes Cr(VI) reduction as shown in Fig. 8a. Djellabi et al. synthesized novel CPs based on the hybridization of Tris(4-carbazoyl-9 ylphenyl)amine (TCTA) with polyvinylpyrrolidone and 4, 4′-bipyridine linker [151]. Such a polymerization results in stable full visible light responsive photoactive polymer. Because TCTA exhibits a highly negative LUMO of 2.48 V at pH 7 much more compared to TiO_2 (0.84 V), it allows a fast thermodynamic photoreduction of Cr(VI). It was found also that Cr(VI) reduction can be occurred at higher pH value up to 8, unlike TiO_2. The same CPs were combined with Fe_3O_4 to obtain a magnetic photocatalyst for easy recovery [41]. In addition, an enhanced Cr(VI) reduction was obtained because of the synergistic redox effects of CPs and Fe_3O_4 (Fig. 8b).

4. Simultaneous removal of Cr(VI) and organic pollutants via photocatalysis

Due to the co-existence of Cr(VI) and organic pollutants in wastewater, the simultaneous removal of them is of particular importance for practical pollutant remediation [158]. However, with the rapid development and refinement of industry, the types of pollutants have also increased sharply. The strong and complex interactions between different organic pollutants and Cr(VI) further complicate the pollution conditions and make them recalcitrant to the traditional treatment

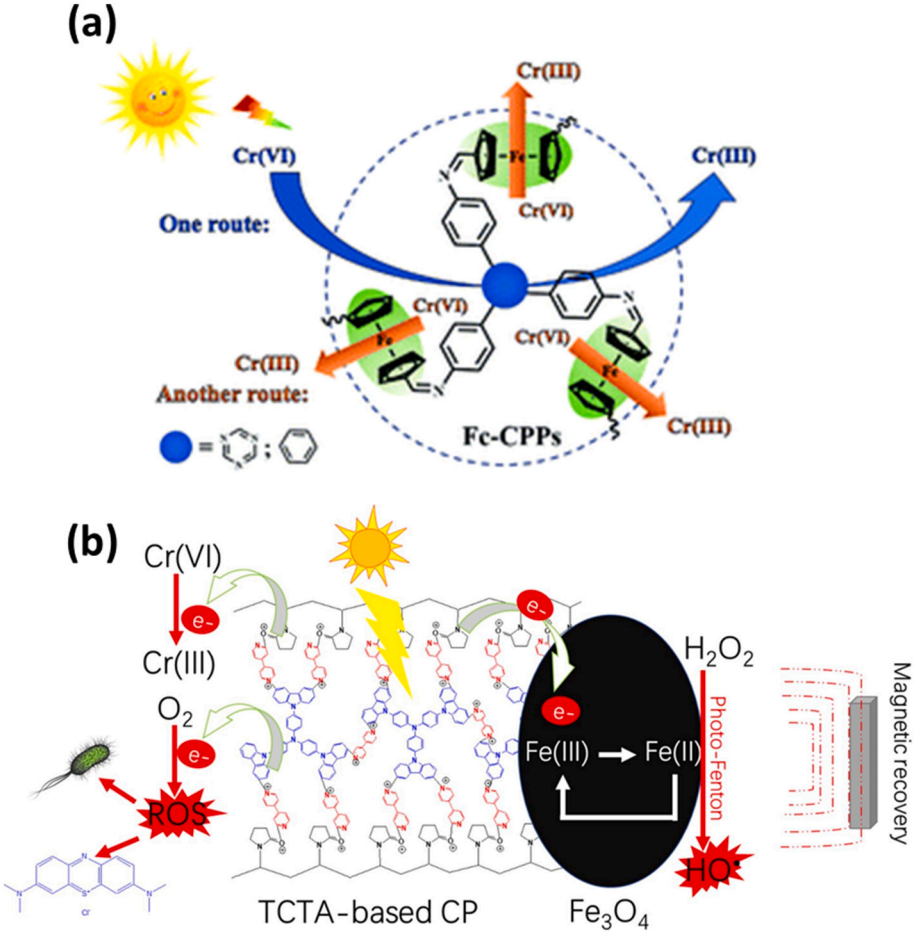

Fig. 8. (a): Ferrocene-containing CPs and ferrocene-free analogue for photocatalytic reduction of Cr(VI), reproduced with permission from [157]. (b): Magnetic recoverable TCTA-PVP based polymer coated Fe_3O_4 for Cr(VI) reduction, bacterial inactivation and dye oxidation, reproduced with permission from [41].

methods [159]. The following sections discuss the simultaneous photoreduction of Cr(VI) and photooxidation of different organic pollutants. Table 2 summarizes the results and main redox species in Cr (VI)/organic pollutants systems.

4.1. Photocatalytic removal of dyes and Cr(VI)

The majority of dye-containing water usually encompasses heavy metal ions, which return to nature as toxic waste [160,161]. The simultaneous photoreduction of Cr(VI) and photooxidation of dyes have been a hot research topic recently. During the oxidation of a dye, it simultaneously plays the role of the hole and ROS scavenger for enhanced Cr(VI) reduction. The oxidation of different dyes during Cr(VI) reduction was studied, such as Luranzol S Kong by TiO_2 [162], methylene blue (MB) by TiO_2 [161], rhodamine B (RhB), crystal violet (CV), methyl orange (MO) by $Cu_2O/BiVO_4$ [163], MB, MO and RhB by Fe-by MOF [164], RhB by g-C_3N_4 [165], RhB by Co-doped $ZnWO_4$ [166], MO or RhB by SnO_2/rGO [167] and so on. Many reports showed that there was an enhancement in the reduction of Cr(VI) and organic dyes because of inhibition of charge recombination [161,168]. The photolysis of dyes might produce excited dye molecules which can participate in the reduction of Cr(VI) [163].

4.2. Photocatalytic removal of phenols and Cr(VI)

Phenol and its derivatives are other typical organic pollutants that widely co-exist in Cr(VI)-containing wastewaters that are discharged from pharmaceutical, printing, textile and petrochemical [169,170]. However, phenol and its derivatives are benzene-containing compounds, and they are more stable than dyes due to the p-orbitals of the benzene ring [171]. More importantly, the adsorption capacity of common adsorbents of phenols is not satisfactory. Owing to their high toxicity, the co-existence of phenols and Cr(VI) is more hazardous to the environment than that of dyes. As a classical photocatalyst, TiO_2-based photocatalysts were firstly employed to remove phenols and Cr(VI) via photocatalysis [172–174]. For instance, CoO_x-loaded TiO_2-based nanosheets were successfully synthesized and used to remove phenol and Cr (VI) under visible light [174]. The results indicated that the highly dispersed CoO_x nanoparticles on the surface of nanosheets significantly improved the removal efficiency of phenol and Cr(VI), which was proved by determining the concentrations of these two contaminants. In addition to TiO_2-based photocatalysts, many other photocatalysts, such as $BiVO_4$ [175], Fe_3O_4/RGO [176], Bi_2WO_6 [177], ZnO [178], g-C_3N_4-based catalysts [179,180] were also used to remediate the contamination of phenols and Cr(VI) simultaneously. In recent years, MOFs were also found to be efficient photocatalysts for this purpose [125,181,182]. Gong et al. [183] fabricated Ag/AgCl/MIL101(Fe) for simultaneous Cr (VI) and phenol oxidation-reduction. The authors disclosed that the reductive quinone derivatives played an important role in reducing Cr (VI) by excluding surface adsorption. Meanwhile, •OH radicals were responsible for phenol oxidization at the initial stage, while $^1O_2$, which evolved from $•O_2^-$ also contributed to the phenol degradation. Additionally, $•O_2^-$ could also gradually cause the accumulation of quinone intermediates and thus, promoting the Cr(VI) reduction. Recently, it was proved that Cr(VI) intermediates, i.e., Cr(V), could participate in the oxidation of organic phenol compounds on the surface of g-C_3N_4 (Fig. 9) [184]. In general, the conversion of Cr(VI) to Cr(V) is unfeasible because of the high energy barrier of 1.40 eV in the mixture of Cr(VI)/phenol, meanwhile, the conversion of Cr(V) to Cr(III) required an energy of 0.34 eV. Therefore, these successive conversion are a limiting step, without additional energy [52]. In photocatalytic system, the energy barrier of Cr(VI)/Cr(III) on the surface of g-C_3N_4 is 0.75 eV. However, after the addition of phenol (BPA), the energy barrier decreased to 0.42 eV, making the conversion thermodynamically faster and easier.

4.3. Photocatalytic removal of pharmaceutical and personal care products (PPCPs) and Cr(VI)

PPCPs are another kind of organic pollutant that has been detected in waterbodies in different countries [185–187]. Particularly, PPCPs in groundwater and surface water pose a great threat to the environment and human health. However, the PPCPs usually occur at very low levels (ppb or ppt), and this makes the traditional methods ineffective at removing them [188]. Several studies have been carried out towards the simultaneous removal of Cr(VI) and PPCPs using photocatalytic technology. Chen et al. [189] successfully prepared a polyaniline-modified MIL-100 (Fe) through ball milling, and the harvested *Z*-scheme MIL-100(Fe)/PANI composite showed outstanding Cr(VI) photoreduction (100 %) and TC photodegradation (84 %) under white light. Ma Ding and co-workers [190] designed a covalent organic framework (COFs) with different heterocyclic nitrogen locations, and the COF was prepared from 3,6- diaminepyridazine (named COF-PDZ) showed excellent Cr(VI) reduction performance due to its stronger affinity to Cr(VI). Besides, COF-PDZ could also inactivate *E. coli* and oxidize paracetamol under visible light. More importantly, the photocatalytic performance of heterocyclic nitrogen-doped COFs can be adjusted by changing the positions and numbers of heterocyclic nitrogen atoms in COFs.

4.4. Photocatalytic reduction of herbicide/pesticides and Cr(VI)

With the continuous growth of the world's population and the gradual improvement of agriculture, pesticides and herbicides are

Table 2
Simultaneous photocatalytic removal of organic pollutants and Cr(VI).

Photocatalyst	Organic pollutant	Light source	Oxidative species	Reductive species	Ref.
TiO_2- Ag@Fe_2O_3	Dye X3B	Xenon	•OH and $•O_2^-$	e^- reduction	[197]
Ag/ZnO@CF	Phenol	Xenon	h^+ and $•O_2^-$	e^- and O_2	[198]
$AgFe_{1-x}Cu_xO_2$ composite	Acid Red G	Vis	h^+ and $•O_2^-$	e^-	[199]
BiOBr/TzDa COF	Rhodamine B	Vis	h^+, •OH and $•O_2^-$	e^-	[200]
Co(II)-Modified TiO_2	bisphenol A	UV	•OH and $•O_2^-$	Co(I) and e^-	[201]
TiO_2 microspheres	Methyl Orange	UV	h^+ and •OH	e^-	[202]
COF	Paracetamol	Vis	$•O_2^-$	e^-	[190]
$AgI/Bi_2Sn_2O_7$	Tetracycline	Vis	h^+, •OH and $•O_2^-$	e^-	[203]
Fluorinated anatase TiO_2	p-Chlorophenol	Vis	h^+	e^-	[204]
Y-Doped TiO_2 nanosheets	Methyl Orange	UV	h^+, •OH and $•O_2^-$	e^-	[205]
CeO_2/g-C_3N_4	2,4-dichlorophenol	Vis	h^+ and •OH	e^-	[206]
$FeWO_4$ nanosheets	acid red G	Vis	•OH and $•O_2^-$	$•CO_2^-$	[207]
Ag/TiO_2 Ag/TiO_2	4-chlorophenol	UV	h^+	Organic by-products and e^-	[207]
hydroxylated -Fe_2O_3	4-Chlorophenol	Vis	•OH, H_2O_2, h^+ and $•O_2^-$	e^- and O_2	[208]
$Cu_2O/BiVO_4$	MB, RhB, CV, MO.	Vis	h^+	e^-	[163]
single crystalline ZnO nanoplates	phenol	UV	h^+	e^-	[178]
B–N–F tri-doped TiO_2	benzoic acid	Vis	Ti^{4+}–O^- oxygen vacancies $•O_2H$ and •OH radicals	Organic by-products and e^-	[209]

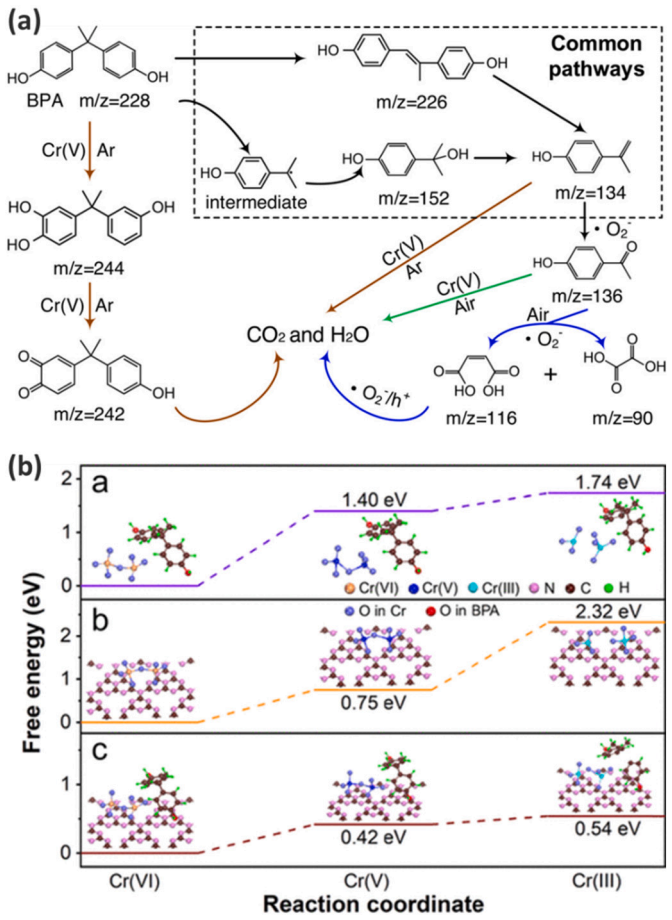

Fig. 9. (a): Role of Cr(V) intermediate for the oxidation BPA in g-C_3N_4 photocatalytic system. (b): Energy barriers of Cr(VI) species, BPA in different systems, a: Cr(VI)/BPA; b: Cr(VI)/g-C_3N_4; and c: Cr(VI)/BPA/g-C_3N_4. Reproduced with permission from ref. [184].

increasingly widely used. However, excess pesticides and herbicides may enter the water body with the scouring of rainwater, resulting in harm to the environment and human health [191–193]. Generally, pesticides are able to eliminate pests, while herbicides specifically eliminate weeds and other unwanted plants. According to the former studies, herbicides and Cr(VI) often coexist in practical wastewater, and thus, developing effective methods for simultaneous removal of them will be of great importance. To address the above concerns, Yang et al. [194] prepared a Bi_2S_3 modified-TiO_2 nanotube (NT) using the pulsed electrodeposition technique. The 3D white fungus-like Bi_2S_3/TiO_2 showed exciting performance in the simultaneous detoxification of 2,4-dichlorophenoxyacetic acid and Cr(VI) under visible light irradiation. The mechanistic study indicated that •OH radicals initiated by photogenerated h^+ played a dominant role in the breaking of the 2,4-D benzene ring, while Cr(VI) was the acceptor for photogenerated e^- and therefore accelerated the degradation of 2,4-D. In another study by Oladipo [195], WO_3/MIL-53(Fe) was synthesized and exhibited remarkable photocatalytic performance in the removal of Cr(VI) and oxidation of 2,4-dichlorophenoxyacetic acid (2,4-D). Their results showed that after 240 min sunlight.

irradiation, 94 % of Cr(VI) reduction was achieved in the presence of WO_3/MIL-53(Fe). Besides, the 2,4-D was degraded by the photo-induced h^+. Most recently, Majhi et al. [196] synthesized two kinds of $CuBi_2O_4$-based heterojunction: $Bi_2O_3/CuBi_2O_4$ (BO/CBO) and $CuO/CuBi_2O_4$ (CO/CBO), for the simultaneous remediation of 17α-ethinylestradiol and Cr(VI). To improve the photocatalytic performance, the two catalysts above were further modified using plasmonic Ag nanoparticles to construct $Bi_2O_3/CuBi_2O_4$/Ag (BO/CBO/Ag) ternary composite material. The degradation efficiency of 17-α Ethinylestradiol (EE2) and Cr(VI) reduction under visible light irradiation by the ternary composite reached 94.6 % and 96.9 %, respectively. The radical analysis indicated that •OH and $•O_2^-$ were identified as the major ROSs towards EE2 oxidation.

5. Analysis of real state of photocatalytic reduction of Cr(VI)

The transfer of a given raised technology is based on several factors such as the effectiveness, the low-cost, the sustainability in comparison to existing technologies. Even though the photocatalytic reduction of Cr (VI) has been widely reported, it transfer to real world application is still not achieved. Certainly, the issue of photocatalytic Cr(VI) reduction is similar to global issue of photocatalytic technology as discussed critically by several authors [70,210], namely slow kinetics, by-products formation, confusion regarding the type of reactor and irradiation light, deactivation of photocatalysts and so on. Therefore, solving most of technology issues of photocatalysis might the transfer of photocatalytic reduction of Cr(VI) as well. However, what are the specific issues of Cr(VI) photoreduction? In terms of kinetics, the reduction of Cr (VI) depends on three factors, one is associated with the activity of the used materials, and as well the pH of solution and the used hole scavenger. The kinetics of Cr(VI) reduction decreases as a function of pH. In addition, the presence of appropriate hole scavenger is very important, which might be an issue at large scale [211]. In terms of reduction ability, some studies showed satisfactory photoreduction of Cr(VI) at reasonable time, while other studies showed slower reactions. The capital issue of photocatalytic Cr(VI) reduction is the deposition of Cr (III) on the surface of the photocatalyst leading to its deactivation. But research studies have reported to overcome this issue as discussed above. Compared to simple adsorption, photocatalytic reduction of Cr (VI) is more effective so far based on many research studies [33,212]. The photocatalytic technology towards Cr(VI) reduction can compete with several existing technologies such as chemical precipitation [213], coagulation and flocculation [214], electrochemical treatments [215], membrane filtration [216], etc. The advantages of those methods are outweighed by critical problems arising: high operational costs, production of sludge, long-term environmental impacts of sludge disposal, and transfer of toxic compounds into a solid phase. Remarkably, the photocatalytic process reduces the development cost by intercepting the use of large amounts of chemicals and introducing easy and unpretentious installation, but still suffering from the efficiency requirements to be immediately amended. More and more efforts are being made to promote the photocatalytic reduction of Cr(VI) to Cr(III). Summarized comparison of photocatalytic technology towards Cr(VI) reduction with other technologies in terms of their assets and liabilities is shown in Table 3. Methods are classified into homogenous and heterogenous. In general, homogenous systems would be costly because of the system is used just once. However, heterogenous systems can be recycled for several times, allowing to reduce the cost of large scale Cr(VI) removal.

6. Conclusions and future trends

The photocatalytic conversion of Cr(VI) into Cr(III) has been one of the hottest research topics over the last decade. Several conclusions could be drawn based on the literature and the real state of using photocatalysis for Cr(VI) photoreduction.

– Among many photocatalytically reducible heavy metals, Cr(VI) has received the greatest attention from the scientific community because of its harmful impact on the environment, animals, and humans. Chromium is classified in group 1 of highly carcinogenic compounds. Furthermore, the geographic distribution of Cr(VI) water pollution affects all the regions. This harassed more research on Cr(VI) photoreduction. Technically, the simplicity in terms of

Table 3
Comparison of Cr(VI) reduction techniques.

Technology		Assets	Liabilities
	Conventional methods		
Coagulation Flocculation	Homogenous	Low capital costs Simplicity and effectiveness Easy operation Relatively simple design Low energy consumption	Toxic of coagulants Sludge production High operation cost Application of chemicals Transfer of metals into solid phase Complexity of scaling
Chemical precipitation	Homogenous	Easy operation Ambient conditions Low capital costs Ease of pH control	Post treatment requirement Toxic sludge production Large amount of chemical use Hazardous storage and chemicals handling
Electrochemical treatment	Homogenous	Easy operation High selectivity Reduced sludge production No additional chemical use	High energy consumption Cell and electrode dependence Post treatment requirement pH control needed
Adsorption	Heterogenous	Availability of adsorbents Easy operation and low cost Relatively simple design	Low selectivity and capacity Complicated reactivation Post treatment requirement Disposal of adsorbents pH control needed
Membrane filtration	Heterogenous	Availability of membranes High selectivity Easy operation	Membrane fouling and clogging High production and operation cost Toxic sludge production High energy consumption
Ion flotation	Heterogenous	Easy operation and flexibility High selectivity Low energy consumption Reduced sludge production	Difficulty in metal ion separation High production and operation cost Complexity of scaling pH control needed
Ion exchange	Heterogenous	Low-cost materials Easy operation Cost-efficiency High selectivity	Low stability and reusability Fouling of exchange matrix High production and operation cost pH control needed
	Modern and promising technologies		
Biosorption	Heterogenous	Simple operation Low sludge production Low operational costs Removal efficiencies and regeneration	pH and temperature control needed High maintenance cost High energy consumption
Electrodialysis	Heterogenous	Reusability of effluent water Rapid removal process Efficiency	Membrane fouling High energy consumption High sludge production
Photocatalysis	Heterogenous	Variety of catalysts No sludge production	pH control needed Catalyst properties

Table 3 (*continued*)

Technology	Assets	Liabilities
	Simple operation and operation cost	influence efficiency Complexity of scaling

analysis of Cr(VI) by direct spectrophotometric approach (with or without the addition of 1,5-Diphenylcarbazide) might have facilitated the immense research studies conducted globally.

- Several classes of photocatalytic materials have been reported for the reduction of Cr(VI). Similar to all photocatalytic studies, predominantly applied approaches, namely doping, heterojunction systems, combination with carbon materials, MOFs and conjugated polymers, and so on, were reported for synergistic or/and enhanced photocatalytic reduction of Cr(VI). In several cases, conjugated polymers have been reported to be excellent photocatalysts for Cr(VI) reduction. However, the stability of most conjugated polymers and light/self-oxidation are serious matters to be taken into consideration.
- MOFs-based photocatalysts showed excellent Cr(VI) photoreduction; however, MOFs suffer from low structural stability, photo-corrosion, poor recycling ability, and unstable crystallinity and periodicity [217]. Therefore, further investigation to understand the parameters to control and prevent the destruction of MOFs.
- The combination of inorganic semiconductors with carbon-based materials can enhance the photocatalytic reduction of Cr(VI) through *Adsorb and shuttle Process*, photosensitizing, and enhanced photo-generated charge separation.
- Another issue of Cr(VI) photocatalytic reduction is the narrowed pH range, as Cr(VI) can be reduced effectively only in an acidic medium. Even though many reported materials can work at higher pH values up to 7, they have slower reduction kinetics. Therefore, the reduction of Cr(VI) in real wastewaters could be limited by the pH. In addition, many classes of photocatalytic materials exhibit high corrosion at low pH, which requires the fabrication of highly stable materials in an acidic medium.
- The development of smart materials/composites exhibiting simultaneously Cr(VI) reduction and organic pollutants degradation is still a challenging hot research area, especially if the photocatalytic tests are carried out to treat real wastewater.
- The produced Cr(III) can be adsorbed on the surface or released from the surface to the solution. The adsorption of Cr(III) on the surface of the photocatalyst could lead to catalyst deactivation. Recovering Cr (III) from the photocatalytic material is quite difficult and costly in some cases. Very few recent studies have edited photocatalytic materials to enhance the selectivity of Cr(VI) and fast desorption of the generated Cr(III).
- The evaluation of the photocatalytic materials used for Cr(VI) reduction should be done under moderated light irradiation that would be similar to real conditions as pollution is reaching surface waters.
- Socio-economic assessments are still missing in order to compare the photocatalytic Cr(VI) reduction process with other available technologies/processes. In addition, computational studies are recommended for predicting the suitable materials and photocatalytic mechanisms.

From our point of view, we believe that optimizing the photocatalytic Cr(VI) reduction should pass by necessary steps. As a future direction, recommendations for the synthesis of cost-effective and efficient materials for sustainable photocatalytic Cr(VI) reduction are summarized in Fig. 10.

Abbreviations

AIS $AgIn_5S_8$

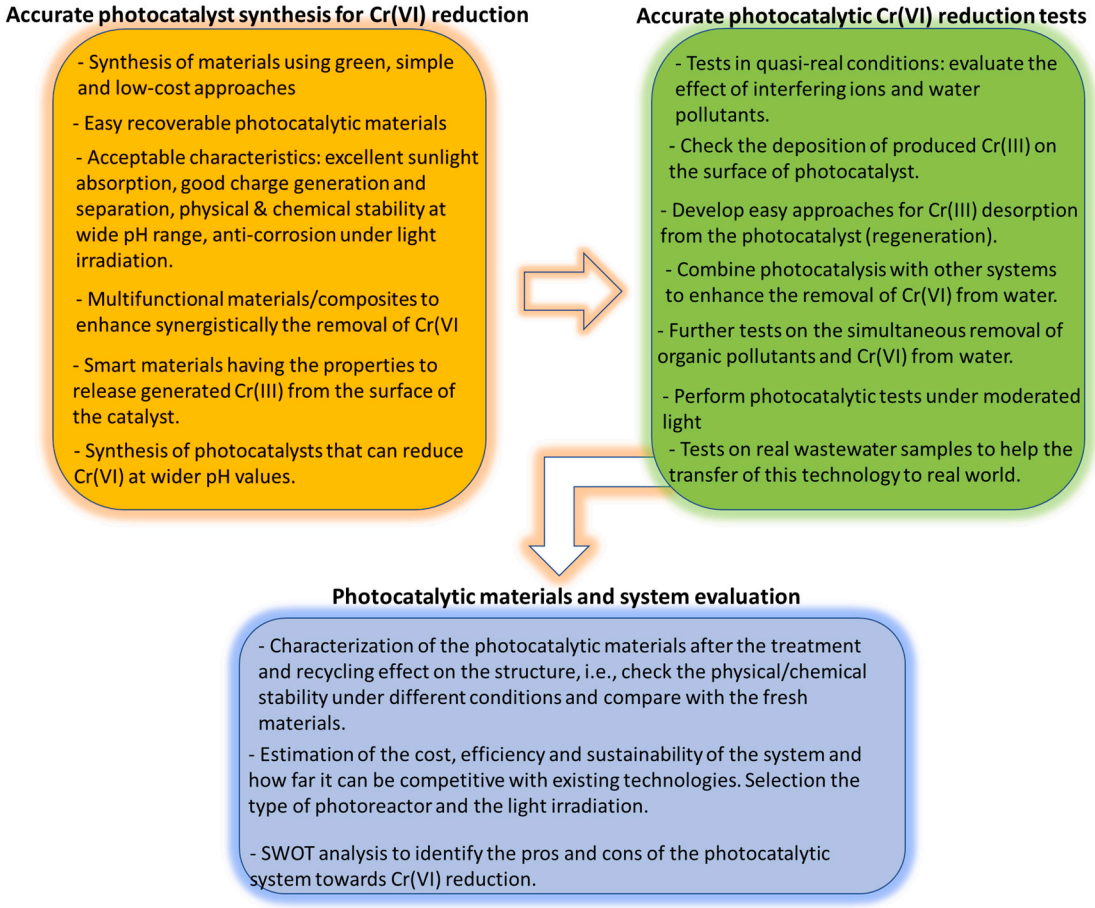

Fig. 10. The scheme shows the accurate synthesis of photocatalytic materials, accurate photocatalytic Cr(VI) reduction, and evaluation of the photocatalytic system after the treatment.

BUC-21	2D coordination polymer of Zn(*bpy*)L (bpy = 4,4′-bipyridine; L = cis-1,3-dibenzyl-2-imidazolidone-4,5-dicarboxylic acid)
CB	conductive band
COFs	covalent organic framework
CPs	conjugated polymers
CQDs	carbon quantum dots
GO	graphene oxide
HOMO	Highest Occupied Molecular Orbital
LSPR	localized surface plasmon resonance
LUMO	lowest unoccupied molecular orbital
MOFs	metal-organic frameworks
NPs	nanoparticles
PCN	polymeric carbon nitride
PPCPs	pharmaceuticals and personal care products
PVP	polyvinylpyrrolidone
ROSs	reactive oxygen species
TC-HCl	tetracycline hydrochloride
TCTA	tris(4-carbazoyl-9-ylphenyl)amine
TCTA	tris(4-carbazoyl-9-ylphenyl)amine
VB	valence band

Declaration of competing interest

The author declares no competing interests.

Data availability

The data that has been used is confidential.

Acknowledgement

Dr. Ridha Djellabi acknowledges Maria Zambrano Grants-2021URV-MZ-15.

References

[1] H. Oliveira, Chromium as an environmental pollutant: insights on induced plant toxicity, J. Bot. 1–8 (2012) 2012.
[2] K.E. Ukhurebor, U.O. Aigbe, R.B. Onyancha, W. Nwankwo, O.A. Osibote, H. K. Paumo, O.M. Ama, C.O. Adetunji, I.U. Siloko, Effect of hexavalent chromium on the environment and removal techniques: a review, J. Environ. Manag. 280 (2021), 111809.
[3] P. Sharma, S.P. Singh, S.K. Parakh, Y.W. Tong, Health hazards of hexavalent chromium (Cr (VI)) and its microbial reduction, Bioengineered 13 (2022) 4923–4938.
[4] A. Zhitkovich, Chromium in drinking water: sources, metabolism, and cancer risks, Chem. Res. Toxicol. 24 (2011) 1617–1629.
[5] W.H. Organization, Chromium in Drinking-water, World Health Organization, 2020.
[6] M.H. Mondal, W. Begum, M. Nasrollahzadeh, F. Ghorbannezhad, V. Antoniadis, E. Levizou, B. Saha, A comprehensive review on chromium chemistry along with detection, speciation, extraction and remediation of hexavalent chromium in contemporary science and technology, Vietnam, J.Chem. 59 (2021) 711–732.
[7] M. Touihri, F. Guesmi, C. Hannachi, B. Hamrouni, L. Sellaoui, M. Badawi, J. Poch, N. Fiol, Single and simultaneous adsorption of Cr (VI) and Cu (II) on a novel Fe3O4/pine cones gel beads nanocomposite: experiments, characterization and isotherms modeling, Chem. Eng. J. 416 (2021), 129101.
[8] Z. Yao, Y. Li, Y. Cui, K. Zheng, B. Zhu, H. Xu, L. Zhu, Tertiary amine block copolymer containing ultrafiltration membrane with pH-dependent macromolecule sieving and Cr (VI) removal properties, Desalination 355 (2015) 91–98.
[9] Y. Ren, Y. Han, X. Lei, C. Lu, J. Liu, G. Zhang, B. Zhang, Q. Zhang, A magnetic ion exchange resin with high efficiency of removing Cr (VI), Colloids Surf. A Physicochem. Eng. Asp. 604 (2020), 125279.

[10] A. Çimen, Removal of chromium from wastewater by reverse osmosis, Russ. J. Phys. Chem. A 89 (2015) 1238–1243.
[11] T. Ölmez, The optimization of Cr (VI) reduction and removal by electrocoagulation using response surface methodology, J. Hazard. Mater. 162 (2009) 1371–1378.
[12] B. Wang, Z. Li, Q. Lang, M. Tan, C. Ratanatamskul, M. Lee, Y. Liu, Y. Zhang, A comprehensive investigation on the components in ionic liquid-based polymer inclusion membrane for Cr (VI) transport during electrodialysis, J. Membr. Sci. 604 (2020), 118016.
[13] C.E. Barrera-Díaz, V. Lugo-Lugo, B. Bilyeu, A review of chemical, electrochemical and biological methods for aqueous Cr (VI) reduction, J. Hazard. Mater. 223 (2012) 1–12.
[14] J. Ali, L. Wang, H. Waseem, R. Djellabi, N. Oladoja, G. Pan, FeS@ rGO nanocomposites as electrocatalysts for enhanced chromium removal and clean energy generation by microbial fuel cell, Chem. Eng. J. 384 (2020), 123335.
[15] G. Mamba, J. Kiwi, C. Pulgarin, R. Sanjines, S. Giannakis, S. Rtimi, Evidence for the degradation of an emerging pollutant by a mechanism involving iso-energetic charge transfer under visible light, Appl. Catal. B Environ. 233 (2018) 175–183.
[16] M. Shams, H. Balouchi, H. Alidadi, F. Asadi, E.K. Goharshadi, S. Rezania, S. Rtimi, I. Anastopoulos, Z. Bonyadi, K. Mehranzamir, Coupling electrocoagulation and solar photocatalysis for electro-and photo-catalytic removal of carmoisine by Ag/graphitic carbon nitride: optimization by process modeling and kinetic studies, J. Mol. Liq. 340 (2021), 116917.
[17] S. Rtimi, C. Pulgarin, R. Sanjines, J. Kiwi, Innovative semi-transparent nanocomposite films presenting photo-switchable behavior and leading to a reduction of the risk of infection under sunlight, RSC Adv. 3 (2013) 16345–16348.
[18] M. Ebrahimi, O. Akhavan, Nanomaterials for photocatalytic degradations of analgesic, mucolytic and anti-biotic/viral/inflammatory drugs widely used in controlling SARS-CoV-2, Catalysts 12 (2022) 667.
[19] J.Y.J. Low, Jaroniec M. Wageh, S. Al-Ghamdi A, Adv. Mater. 29 (2017), 1601694.
[20] A. Hajjaji, M. Elabidi, K. Trabelsi, A. Assadi, B. Bessais, S. Rtimi, Bacterial adhesion and inactivation on Ag decorated TiO2-nanotubes under visible light: effect of the nanotubes geometry on the photocatalytic activity, Colloids Surf. B: Biointerfaces 170 (2018) 92–98.
[21] C. Mondal, M. Ganguly, J. Pal, A. Roy, J. Jana, T. Pal, Morphology controlled synthesis of SnS2 nanomaterial for promoting photocatalytic reduction of aqueous Cr (VI) under visible light, Langmuir 30 (2014) 4157–4164.
[22] I.A. Abdelhafeez, S. Ramakrishna, Promising sustainable models toward water, air, and solid sustainable management in the view of SDGs, Mater. Circ. Econ. 3 (2021) 1–10.
[23] R. Djellabi, F.M. Ghorab, S. Nouacer, A. Smara, O. Khireddine, Cr (VI) photocatalytic reduction under sunlight followed by Cr (III) extraction from TiO2 surface, Mater. Lett. 176 (2016) 106–109.
[24] H. Wei, Q. Zhang, Y. Zhang, Z. Yang, A. Zhu, D.D. Dionysiou, Enhancement of the Cr (VI) adsorption and photocatalytic reduction activity of g-C3N4 by hydrothermal treatment in HNO3 aqueous solution, Appl. Catal. A Gen. 521 (2016) 9–18.
[25] M. Shirzad Siboni, M. Samadi, J. Yang, S. Lee, Photocatalytic reduction of Cr (VI) and Ni (II) in aqueous solution by synthesized nanoparticle ZnO under ultraviolet light irradiation: a kinetic study, Environ. Technol. 32 (2011) 1573–1579.
[26] R. Djellabi, X. Zhao, M.F. Ordonez, E. Falletta, C.L. Bianchi, Comparison of the photoactivity of several semiconductor oxides in floating aerogel and suspension systems towards the reduction of Cr (VI) under visible light, Chemosphere 281 (2021), 130839.
[27] A. Amirulsyafiee, M.M. Khan, A. Khan, M.Y. Khan, M.H. Harunsani, Influence of Zr doping on Ag3PO4 for photocatalytic degradation of dyes and Cr (VI) reduction under visible light irradiation, Mater. Chem. Phys. 291 (2022), 126673.
[28] V. Bortolotto, R. Djellabi, A. Giordana, G. Cerrato, A. Di Michele, C.L. Bianchi, Photocatalytic behaviour of Ag3PO4, Fe3O4 and Ag3PO4/Fe3O4 heterojunction towards the removal of organic pollutants and Cr (VI) from water: efficiency and light-corrosion deactivation, Inorg. Chem. Commun. 141 (2022), 109516.
[29] R. Gherbi, N. Nasrallah, A. Amrane, R. Maachi, M. Trari, Photocatalytic reduction of Cr (VI) on the new hetero-system CuAl2O4/TiO2, J. Hazard. Mater. 186 (2011) 1124–1130.
[30] Z. Wei, N. Zheng, X. Dong, X. Zhang, H. Ma, X. Zhang, M. Xue, Green and controllable synthesis of one-dimensional Bi2O3/BiOI heterojunction for highly efficient visible-light-driven photocatalytic reduction of Cr (VI), Chemosphere 257 (2020), 127210.
[31] J. Pan, Z. Guan, J. Yang, Q. Li, Facile fabrication of ZnIn2S4/SnS2 3D heterostructure for efficient visible-light photocatalytic reduction of Cr (VI), Chin. J. Catal. 41 (2020) 200–208.
[32] Z. Gao, H. Yang, X. Fu, Q. Jin, Q. Wu, L. Kang, J. Wu, Efficient photoreduction of Cr (VI) on TiO2/functionalized activated carbon (TiO2/AC-AEMP): improved adsorption of Cr (VI) and induced transfer of electrons, Environ. Sci. Pollut. Res. 27 (2020) 17446–17457.
[33] R. Djellabi, M.Fouzi Ghorab, C.L. Bianchi, G. Cerrato, S. Morandi, Removal of Crystal Violet and Hexavalent Chromium Using TiO2-bentonite Under Sunlight: Effect of TiO2 Content, 2016.
[34] R. Djellabi, C.L. Bianchi, M.R. Haider, J. Ali, E. Falletta, M.F. Ordonez, A. Bruni, M. Sartirana, R. Geioushy, in: Photoactive Polymer for Wastewater Treatment, Nanomaterials for Water Treatment and Remediation, CRC Press, 2021, pp. 217–244.
[35] R. Djellabi, J. Ali, X. Zhao, A.N. Saber, B. Yang, CuO NPs incorporated into electron-rich TCTA@ PVP photoactive polymer for the photocatalytic oxidation of dyes and bacteria inactivation, J.Water Process Eng. 36 (2020), 101238.
[36] Y. Zhang, M. Xu, H. Li, H. Ge, Z. Bian, The enhanced photoreduction of Cr (VI) to Cr (III) using carbon dots coupled TiO2 mesocrystals, Appl. Catal. B Environ. 226 (2018) 213–219.
[37] A. Bhati, S.R. Anand, D. Saini, S.K. Sonkar, Sunlight-induced photoreduction of Cr (VI) to Cr (III) in wastewater by nitrogen-phosphorus-doped carbon dots, npj cleanWater 2 (2019) 1–9.
[38] J.J. Testa, M.A. Grela, M.I. Litter, Experimental evidence in favor of an initial one-electron-transfer process in the heterogeneous photocatalytic reduction of chromium (VI) over TiO2, Langmuir 17 (2001) 3515–3517.
[39] J.J. Testa, M.A. Grela, M.I. Litter, Heterogeneous photocatalytic reduction of chromium (VI) over TiO2 particles in the presence of oxalate: involvement of Cr (V) species, Environ.Sci.Technol. 38 (2004) 1589–1594.
[40] J.M. Meichtry, M. Brusa, G. Mailhot, M.A. Grela, M.I. Litter, Heterogeneous photocatalysis of Cr (VI) in the presence of citric acid over TiO2 particles: relevance of Cr (V)–citrate complexes, Appl. Catal. B Environ. 71 (2007) 101–107.
[41] R. Djellabi, J. Ali, B. Yang, M.R. Haider, P. Su, C.L. Bianchi, X. Zhao, Synthesis of magnetic recoverable electron-rich TCTA@ PVP based conjugated polymer for photocatalytic water remediation and disinfection, Sep. Purif. Technol. 250 (2020), 116954.
[42] R. Djellabi, M. Ghorab, Photoreduction of toxic chromium using TiO2-immobilized under natural sunlight: effects of some hole scavengers and process parameters, Desalin. Water Treat. 55 (2015) 1900–1907.
[43] B.A. Marinho, R.O. Cristóvão, R. Djellabi, J.M. Loureiro, R.A. Boaventura, V. J. Vilar, Photocatalytic reduction of Cr (VI) over TiO2-coated cellulose acetate monolithic structures using solar light, Appl. Catal. B Environ. 203 (2017) 18–30.
[44] D. Chen, A.K. Ray, Removal of toxic metal ions from wastewater by semiconductor photocatalysis, Chem. Eng. Sci. 56 (2001) 1561–1570.
[45] M. Valari, A. Antoniadis, D. Mantzavinos, I. Poulios, Photocatalytic reduction of Cr (VI) over titania suspensions, Catal. Today 252 (2015) 190–194.
[46] D.-S. An, H.-Y. Zeng, G.-F. Xiao, J. Xiong, C.-R. Chen, G. Hu, Cr (VI) reduction over Ag3PO4/g-C3N4 composite with pn heterostructure under visible-light irradiation, J. Taiwan Inst. Chem. Eng. 117 (2020) 133–143.
[47] V. Hasija, P. Raizada, P. Singh, N. Verma, A.A.P. Khan, A. Singh, R. Selvasembian, S.Y. Kim, C.M. Hussain, V.-H. Nguyen, Progress on the photocatalytic reduction of hexavalent Cr (VI) using engineered graphitic carbon nitride, Process Saf. Environ. Prot. 152 (2021) 663–678.
[48] Y. Deng, L. Tang, G. Zeng, Z. Zhu, M. Yan, Y. Zhou, J. Wang, Y. Liu, J. Wang, Insight into highly efficient simultaneous photocatalytic removal of Cr (VI) and 2, 4-diclorophenol under visible light irradiation by phosphorus doped porous ultrathin g-C3N4 nanosheets from aqueous media: performance and reaction mechanism, Appl. Catal. B Environ. 203 (2017) 343–354.
[49] F.V. Hackbarth, D. Maass, A.A.U. de Souza, V.J. Vilar, S.M.G.U. de Souza, Removal of hexavalent chromium from electroplating wastewaters using marine macroalga Pelvetia canaliculata as natural electron donor, Chem. Eng. J. 290 (2016) 477–489.
[50] W. Zhao, B. Bai, Z. Hong, X. Zhang, B. Zhou, Berbamine (BBM), a natural STAT3 inhibitor, synergistically enhances the antigrowth and proapoptotic effects of sorafenib on hepatocellular carcinoma cells, ACS Omega 5 (2020) 24838–24847.
[51] Z. Kang, H. Gao, Z. Hu, X. Jia, D. Wen, Ni–Fe/reduced graphene oxide nanocomposites for hexavalent chromium reduction in an aqueous environment, ACS Omega 7 (2022) 4041–4051.
[52] C.M. Stern, T.O. Jegede, V.A. Hulse, N. Elgrishi, Electrochemical reduction of Cr (VI) in water: lessons learned from fundamental studies and applications, Chem. Soc. Rev. 50 (2021) 1642–1667.
[53] V.N. Montesinos, C. Salou, J.M. Meichtry, C. Colbeau-Justinc, M.I. Litter, Role of Cr (III) deposition during the photocatalytic transformation of hexavalent chromium and citric acid over commercial TiO2 samples, Photochem. Photobiol. Sci. 15 (2016) 228–234.
[54] Y. Li, Y. Bian, H. Qin, Y. Zhang, Z. Bian, Photocatalytic reduction behavior of hexavalent chromium on hydroxyl modified titanium dioxide, Appl. Catal. B Environ. 206 (2017) 293–299.
[55] E.T. Anthony, N.A. Oladoja, Process enhancing strategies for the reduction of Cr (VI) to Cr (III) via photocatalytic pathway, Environ. Sci. Pollut. Res. (2021) 1–28.
[56] B.A. Marinho, R. Djellabi, R.O. Cristóvão, J.M. Loureiro, R.A. Boaventura, M. M. Dias, J.C.B. Lopes, V.J. Vilar, Intensification of heterogeneous TiO2 photocatalysis using an innovative micro–meso-structured-reactor for Cr (VI) reduction under simulated solar light, Chem. Eng. J. 318 (2017) 76–88.
[57] H. Karimi-Maleh, A. Ayati, S. Ghanbari, Y. Orooji, B. Tanhaei, F. Karimi, M. Alizadeh, J. Rouhi, L. Fu, M. Sillanpää, Recent advances in removal techniques of Cr (VI) toxic ion from aqueous solution: a comprehensive review, J. Mol. Liq. 329 (2021), 115062.
[58] V. Poliukhova, J.-K. Park, D. Kim, S. Khan, J.Y. Seo, S.J. Kim, G.-H. Moon, K.-Y. Baek, S. Kim, S.-H. Cho, Rational design of dynamic Z-scheme heterojunction composites for photocatalytic Cr(VI) reduction and H2 production: an experimental and computational study, Chem.Eng.J.Adv. 12 (2022), 100363.
[59] C. Xu, P. Zhao, M. Cai, Z. Dan, S. Zeng, J. Du, P. Yang, J. Xiong, Enhanced photocatalytic reduction of Cr (VI) by Cu2O/Bi5O7I microrods composites under visible light, J. Photochem. Photobiol. A Chem. 395 (2020), 112495.
[60] J. Zhang, W. Zhang, F. Yuan, Z. Yang, J. Lin, Y. Huang, M. Ding, Effect of Bi5O7I/calcined ZnAlBi-LDHs composites on Cr (VI) removal via adsorption and photocatalytic reduction, Appl. Surf. Sci. 562 (2021), 150129.
[61] J. Ren, T. Hu, Q. Gong, Q. Wang, B. Sun, T. Gao, P. Cao, G. Zhou, Spherical Bi2WO6/Bi2S3/MoS2 np heterojunction with excellent visible-light photocatalytic reduction Cr (VI) activity, Nanomaterials 10 (2020) 1813.

[62] Z. Wu, Z. Li, M. Wu, J. Shen, W. Feng, X. Li, D. Xu, S. Zhang, N. Ma, Defective BiO2-x/BiOCl porous ultrathin nanosheets for efficient solar-light-driven photoreduction of Cr (VI), Mater. Sci. Semicond. Process. 128 (2021), 105781.
[63] D. Wang, M. Cao, Y. Feng, J. Yao, Self-assembly of ZnIn2S4 nanosheets on g-C3N4 nanotubes for efficient photocatalytic reduction of Cr (VI), Microporous Mesoporous Mater. 330 (2022), 111598.
[64] Q. Wang, X. Shi, J. Xu, J.C. Crittenden, E. Liu, Y. Zhang, Y. Cong, Highly enhanced photocatalytic reduction of Cr (VI) on AgI/TiO2 under visible light irradiation: influence of calcination temperature, J. Hazard. Mater. 307 (2016) 213–220.
[65] S. Li, C. Wang, M. Cai, F. Yang, Y. Liu, J. Chen, P. Zhang, X. Li, X. Chen, Facile fabrication of TaON/Bi2MoO6 core–shell S-scheme heterojunction nanofibers for boosting visible-light catalytic levofloxacin degradation and Cr (VI) reduction, Chem. Eng. J. 428 (2022), 131158.
[66] Z. Lin, Y. Zheng, F. Deng, X. Luo, J. Zou, P. Shao, S. Zhang, H. Tang, Target-directed design of dual-functional Z-scheme AgIn5S8/SnS2 heterojunction for Pb (II) capture and photocatalytic reduction of Cr (VI): performance and mechanism insight, Sep. Purif. Technol. 277 (2021), 119430.
[67] R. Djellabi, M. Fouzi Ghorab, A. Smara, C.L. Bianchi, G. Cerrato, X. Zhao, B. Yang, Titania-Montmorillonite for the photocatalytic removal of contaminants from water: adsorb & shuttle process, in: Green Materials for Wastewater Treatment, Springer, 2020, pp. 291–319.
[68] A.N. Saber, R. Djellabi, I. Fellah, N. Abderrahim, C.L. Bianchi, Synergistic sorption/photo-Fenton removal of typical substituted and parent polycyclic aromatic hydrocarbons from coking wastewater over CuO-Montmorillonite, J. Water Process Eng. 44 (2021), 102377.
[69] I. Fellah, R. Djellabi, H.B. Amor, N. Abderrahim, C.L. Bianchi, A. Giordana, G. Cerrato, A. Di Michele, N. Hamdi, Visible light responsive heterostructure HTDMA-BiPO4 modified clays for effective diclofenac sodium oxidation: role of interface interactions and basal spacing, J.Water Process Eng. 48 (2022), 102788.
[70] R. Djellabi, R. Giannantonio, E. Falletta, C.L. Bianchi, SWOT analysis of photocatalytic materials towards large scale environmental remediation, Curr. Opin. Chem. Eng. 33 (2021), 100696.
[71] A. Cox, P. Venkatachalam, S. Sahi, N. Sharma, Silver and titanium dioxide nanoparticle toxicity in plants: a review of current research, Plant Physiol. Biochem. 107 (2016) 147–163.
[72] E. Friehs, Y. AlSalka, R. Jonczyk, A. Lavrentieva, A. Jochums, J.-G. Walter, F. Stahl, T. Scheper, D. Bahnemann, Toxicity, phototoxicity and biocidal activity of nanoparticles employed in photocatalysis, J. Photochem. Photobiol. C: Photochem. Rev. 29 (2016) 1–28.
[73] L. Zhang, C. Chuaicham, V. Balakumar, B. Ohtani, K. Sasaki, Fabrication of adsorbed Fe (III) and structurally doped Fe (III) in montmorillonite/TiO2 composite for photocatalytic degradation of phenol, Minerals 11 (2021) 1381.
[74] N. Abderrahim, R. Djellabi, H.B. Amor, I. Fellah, A. Giordana, G. Cerrato, A. Di Michele, C.L. Bianchi, Sustainable purification of phosphoric acid contaminated with Cr (VI) by Ag/Ag3PO4 coated activated carbon/montmorillonite under UV and solar light: materials design and photocatalytic mechanism, J.Environ.Chem. Eng. 10 (2022), 107870.
[75] X. Liu, L. Pan, T. Lv, T. Lu, G. Zhu, Z. Sun, C. Sun, Microwave-assisted synthesis of ZnO–graphene composite for photocatalytic reduction of Cr(VI), Catal. Sci. Technol. 1 (2011) 1189–1193.
[76] L. Liu, C. Luo, J. Xiong, Z. Yang, Y. Zhang, Y. Cai, H. Gu, Reduced graphene oxide (rGO) decorated TiO2 microspheres for visible-light photocatalytic reduction of Cr (VI), J. Alloys Compd. 690 (2017) 771–776.
[77] R. Djellabi, B. Yang, K. Xiao, Y. Gong, D. Cao, H.M.A. Sharif, X. Zhao, C. Zhu, J. Zhang, Unravelling the mechanistic role of TiOC bonding bridge at titania/lignocellulosic biomass interface for Cr (VI) photoreduction under visible light, J. Colloid Interface Sci. 553 (2019) 409–417.
[78] Y. Wang, S. Chen, D. Jin, A. Gong, X. Xu, C. Wu, Facile one-step solvothermal synthesis of active carbon/BiOI microspheres with enhanced visible light-driven photocatalytic activity in the reduction of Cr(vi), RSC Adv. 8 (2018) 7518–7522.
[79] U. Alam, K. Pandey, N. Verma, Photocatalytic oxidation of glyphosate and reduction of Cr (VI) in water over ACF-supported CoNiWO4-gCN composite under batch and flow conditions, Chemosphere 297 (2022), 134119.
[80] H. Mekatel, S. Amokrane, B. Bellal, M. Trari, D. Nibou, Photocatalytic reduction of Cr (VI) on nanosized Fe2O3 supported on natural Algerian clay: characteristics, kinetic and thermodynamic study, Chem. Eng. J. 200 (2012) 611–618.
[81] X. Liu, L. Pan, T. Lv, G. Zhu, Z. Sun, C. Sun, Microwave-assisted synthesis of CdS–reduced graphene oxide composites for photocatalytic reduction of Cr(VI), Chem. Commun. 47 (2011) 11984–11986.
[82] F.T. Johra, W.-G. Jung, RGO–TiO2–ZnO composites: synthesis, characterization, and application to photocatalysis, Appl. Catal. A Gen. 491 (2015) 52–57.
[83] K. Qi, R. Selvaraj, T. Al Fahdi, S. Al-Kindy, Y. Kim, G.-C. Wang, C.-W. Tai, M. Sillanpää, Enhanced photocatalytic activity of anatase-TiO2 nanoparticles by fullerene modification: a theoretical and experimental study, Appl. Surf. Sci. 387 (2016) 750–758.
[84] M.-M. Titirici, R.J. White, N. Brun, V.L. Budarin, D.S. Su, F. del Monte, J.H. Clark, M.J. MacLachlan, Sustainable carbon materials, Chem. Soc. Rev. 44 (2015) 250–290.
[85] R. Leary, A. Westwood, Carbonaceous nanomaterials for the enhancement of TiO2 photocatalysis, Carbon 49 (2011) 741–772.
[86] R. Djellabi, B. Yang, H.M.A. Sharif, J. Zhang, J. Ali, X. Zhao, Sustainable and easy recoverable magnetic TiO2-Lignocellulosic Biomass@ Fe3O4 for solar photocatalytic water remediation, J. Clean. Prod. 233 (2019) 841–847.
[87] R.B. Marcelino, C.C. Amorim, Towards visible-light photocatalysis for environmental applications: band-gap engineering versus photons absorption—a review, Environ. Sci. Pollut. Res. 26 (2019) 4155–4170.
[88] J. Suave, S.M. Amorim, J. Angelo, L. Andrade, A. Mendes, R.F. Moreira, TiO2/reduced graphene oxide composites for photocatalytic degradation in aqueous and gaseous medium, J. Photochem. Photobiol. A Chem. 348 (2017) 326–336.
[89] S. Morales-Torres, L.M. Pastrana-Martínez, J.L. Figueiredo, J.L. Faria, A.M. Silva, Design of graphene-based TiO2 photocatalysts—a review, Environ. Sci. Pollut. Res. 19 (2012) 3676–3687.
[90] R. Djellabi, B. Yang, Y. Wang, X. Cui, X. Zhao, Carbonaceous biomass-titania composites with TiOC bonding bridge for efficient photocatalytic reduction of Cr (VI) under narrow visible light, Chem. Eng. J. 366 (2019) 172–180.
[91] P. Song, X. Zhang, M. Sun, X. Cui, Y. Lin, Graphene oxide modified TiO 2 nanotube arrays: enhanced visible light photoelectrochemical properties, Nanoscale 4 (2012) 1800–1804.
[92] Z. Li, B. Gao, G.Z. Chen, R. Mokaya, S. Sotiropoulos, G.L. Puma, Carbon nanotube/titanium dioxide (CNT/TiO2) core–shell nanocomposites with tailored shell thickness, CNT content and photocatalytic/photoelectrocatalytic properties, Appl. Catal. B Environ. 110 (2011) 50–57.
[93] M. Shaban, A.M. Ashraf, M.R. Abukhadra, TiO2 nanoribbons/carbon nanotubes composite with enhanced photocatalytic activity; fabrication, characterization, and application, Sci. Rep. 8 (2018) 1–17.
[94] G.D. Tarigh, F. Shemirani, N.S. Maz'hari, Fabrication of a reusable magnetic multi-walled carbon nanotube–TiO 2 nanocomposite by electrostatic adsorption: enhanced photodegradation of malachite green, RSC Adv. 5 (2015) 35070–35079.
[95] D. Meroni, R. Djellabi, M. Ashokkumar, C.L. Bianchi, D.C. Boffito, Sonoprocessing: from concepts to large-scale reactors, Chem. Rev. 122 (2021) 3219–3258.
[96] C. Wang, G. Guo, P. Wang, Two sodium and lanthanide (III) MOFs based on oxalate and V-shaped 4, 4′-oxybis (benzoate) ligands: hydrothermal synthesis, crystal structure, and luminescence properties, J. Mol. Struct. 1032 (2013) 93–99.
[97] C. Wang, Z. Wang, F. Gu, G. Guo, Three novel lanthanide MOFs constructed from 1, 3-benzenedicarboxylic acid and 1, 10-phenanthroline: hydrothermal synthesis, crystal structure and thermal properties, J. Mol. Struct. 1004 (2011) 39–44.
[98] M. Fuentes-Cabrera, D.M. Nicholson, B.G. Sumpter, M. Widom, Electronic structure and properties of isoreticular metal-organic frameworks: the case of M-IRMOF1 (M= Zn, Cd, Be, Mg, and Ca), J. Chem. Phys. 123 (2005), 124713.
[99] L. Shen, W. Wu, R. Liang, R. Lin, L. Wu, Highly dispersed palladium nanoparticles anchored on UiO-66 (NH 2) metal-organic framework as a reusable and dual functional visible-light-driven photocatalyst, Nanoscale 5 (2013) 9374–9382.
[100] C.-Y. Sun, S.-X. Liu, D.-D. Liang, K.-Z. Shao, Y.-H. Ren, Z.-M. Su, Highly stable crystalline catalysts based on a microporous metal– organic framework and polyoxometalates, J. Am. Chem. Soc. 131 (2009) 1883–1888.
[101] R.Q. Zou, H. Sakurai, Q. Xu, Preparation, adsorption properties, and catalytic activity of 3D porous metal–organic frameworks composed of cubic building blocks and alkali-metal ions, Angew. Chem. 118 (2006) 2604–2608.
[102] P. Horcajada, C. Serre, G. Maurin, N.A. Ramsahye, F. Balas, M. Vallet-Regí, M. Sebban, F. Taulelle, G. Férey, Flexible porous metal-organic frameworks for a controlled drug delivery, J. Am. Chem. Soc. 130 (2008) 6774–6780.
[103] J.-R. Li, Y. Ma, M.C. McCarthy, J. Sculley, J. Yu, H.-K. Jeong, P.B. Balbuena, H.-C. Zhou, Carbon dioxide capture-related gas adsorption and separation in metal-organic frameworks, Coord. Chem. Rev. 255 (2011) 1791–1823.
[104] H. Kim, D.G. Samsonenko, M. Yoon, J.W. Yoon, Y.K. Hwang, J.-S. Chang, K. Kim, Temperature-triggered gate opening for gas adsorption in microporous manganese formate, Chem. Commun. (2008) 4697–4699.
[105] A. Crake, K.C. Christoforidis, A. Kafizas, S. Zafeiratos, C. Petit, CO2 capture and photocatalytic reduction using bifunctional TiO2/MOF nanocomposites under UV–vis irradiation, Appl. Catal. B Environ. 210 (2017) 131–140.
[106] Y.B. Zhang, W.X. Zhang, F.Y. Feng, J.P. Zhang, X.M. Chen, A highly connected porous coordination polymer with unusual channel structure and sorption properties, Angew. Chem. Int. Ed. 48 (2009) 5287–5290.
[107] V. Kumar, V. Singh, K.-H. Kim, E.E. Kwon, S.A. Younis, Metal-organic frameworks for photocatalytic detoxification of chromium and uranium in water, Coord. Chem. Rev. 447 (2021), 214148.
[108] C.-C. Wang, X.-D. Du, J. Li, X.-X. Guo, P. Wang, J. Zhang, Photocatalytic Cr (VI) reduction in metal-organic frameworks: a mini-review, Appl. Catal. B Environ. 193 (2016) 198–216.
[109] J. Qiu, X.-F. Zhang, X. Zhang, Y. Feng, Y. Li, L. Yang, H. Lu, J. Yao, Constructing Cd0. 5Zn0. 5S@ ZIF-8 nanocomposites through self-assembly strategy to enhance Cr (VI) photocatalytic reduction, J. Hazard. Mater. 349 (2018) 234–241.
[110] H. Li, M. Eddaoudi, M. O'Keeffe, O.M. Yaghi, Design and synthesis of an exceptionally stable and highly porous metal-organic framework, Nature 402 (1999) 276–279.
[111] J.-L. Wang, C. Wang, W. Lin, Metal–organic frameworks for light harvesting and photocatalysis, ACS Catal. 2 (2012) 2630–2640.
[112] J. Long, S. Wang, Z. Ding, S. Wang, Y. Zhou, L. Huang, X. Wang, Amine-functionalized zirconium metal–organic framework as efficient visible-light photocatalyst for aerobic organic transformations, Chem. Commun. 48 (2012) 11656–11658.
[113] C.-C. Wang, Y.-Q. Zhang, J. Li, P. Wang, Photocatalytic CO2 reduction in metal–organic frameworks: a mini review, J. Mol. Struct. 1083 (2015) 127–136.
[114] Y. Horiuchi, T. Toyao, M. Saito, K. Mochizuki, M. Iwata, H. Higashimura, M. Anpo, M. Matsuoka, Visible-light-promoted photocatalytic hydrogen production by using an amino-functionalized Ti (IV) metal–organic framework, J. Phys. Chem. C 116 (2012) 20848–20853.

[115] H. Wang, X. Yuan, Y. Wu, G. Zeng, X. Chen, L. Leng, Z. Wu, L. Jiang, H. Li, Facile synthesis of amino-functionalized titanium metal-organic frameworks and their superior visible-light photocatalytic activity for Cr (VI) reduction, J. Hazard. Mater. 286 (2015) 187–194.
[116] F. Jing, R. Liang, J. Xiong, R. Chen, S. Zhang, Y. Li, L. Wu, MIL-68 (Fe) as an efficient visible-light-driven photocatalyst for the treatment of a simulated waste-water contain Cr (VI) and Malachite Green, Appl. Catal. B Environ. 206 (2017) 9–15.
[117] P. Mahata, G. Madras, S. Natarajan, Novel photocatalysts for the decomposition of organic dyes based on metal-organic framework compounds, J. Phys. Chem. B 110 (2006) 13759–13768.
[118] L. Shen, S. Liang, W. Wu, R. Liang, L. Wu, Multifunctional NH 2-mediated zirconium metal–organic framework as an efficient visible-light-driven photocatalyst for selective oxidation of alcohols and reduction of aqueous Cr(vi), Dalton Trans. 42 (2013) 13649–13657.
[119] L. Shi, T. Wang, H. Zhang, K. Chang, X. Meng, H. Liu, J. Ye, An amine-functionalized iron (III) metal–organic framework as efficient visible-light photocatalyst for Cr (VI) reduction, Adv.Sci. 2 (2015), 1500006.
[120] H.-Q. Zheng, X.-H. He, Y.-N. Zeng, W.-H. Qiu, J. Chen, G.-J. Cao, R.-G. Lin, Z.-J. Lin, B. Chen, Boosting the photoreduction activity of Cr (vi) in metal–organic frameworks by photosensitiser incorporation and framework ionization, J. Mater. Chem. A 8 (2020) 17219–17228.
[121] C. Zhao, Z. Wang, X. Li, X. Yi, H. Chu, X. Chen, C.-C. Wang, Facile fabrication of BUC-21/Bi24O31Br 10 composites for enhanced photocatalytic Cr (VI) reduction under white light, Chem. Eng. J. 389 (2020), 123431.
[122] R. Liang, F. Jing, L. Shen, N. Qin, L. Wu, M@ MIL-100 (Fe)(M= Au, Pd, Pt) nanocomposites fabricated by a facile photodeposition process: efficient visible-light photocatalysts for redox reactions in water, Nano Res. 8 (2015) 3237–3249.
[123] P. Wang, B. Huang, Y. Dai, M.-H. Whangbo, Plasmonic photocatalysts: harvesting visible light with noble metal nanoparticles, Phys. Chem. Chem. Phys. 14 (2012) 9813–9825.
[124] R. Lin, S. Li, J. Wang, J. Xu, C. Xu, J. Wang, C. Li, Z. Li, Facile generation of carbon quantum dots in MIL-53 (Fe) particles as localized electron acceptors for enhancing their photocatalytic Cr (VI) reduction, Inorg. Chem. Front. 5 (2018) 3170–3177.
[125] F. Zhao, Y. Liu, S.B. Hammouda, B. Doshi, N. Guijarro, X. Min, C.-J. Tang, M. Sillanpää, K. Sivula, S. Wang, MIL-101 (Fe)/g-C3N4 for enhanced visible-light-driven photocatalysis toward simultaneous reduction of Cr (VI) and oxidation of bisphenol A in aqueous media, Appl. Catal. B Environ. 272 (2020), 119033.
[126] W. Huang, N. Liu, X. Zhang, M. Wu, L. Tang, Metal organic framework g-C3N4/MIL-53 (Fe) heterojunctions with enhanced photocatalytic activity for Cr (VI) reduction under visible light, Appl. Surf. Sci. 425 (2017) 107–116.
[127] X.-H. Yi, S.-Q. Ma, X.-D. Du, C. Zhao, H. Fu, P. Wang, C.-C. Wang, The facile fabrication of 2D/3D Z-scheme g-C3N4/UiO-66 heterojunction with enhanced photocatalytic Cr (VI) reduction performance under white light, Chem. Eng. J. 375 (2019), 121944.
[128] X.H. Yi, F.X. Wang, X.D. Du, P. Wang, C.C. Wang, Facile fabrication of BUC-21/g-C3N4 composites and their enhanced photocatalytic Cr (VI) reduction performances under simulated sunlight, Appl. Organomet. Chem. 33 (2019), e4621.
[129] J. Ren, S. Lv, S. Wang, M. Bao, X. Zhang, Y. Gao, Y. Liu, Z. Zhang, L. Zeng, J. Ke, Construction of efficient g-C3N4/NH2-UiO-66 (Zr) heterojunction photocatalysts for wastewater purification, Sep. Purif. Technol. 274 (2021), 118973.
[130] L. Shen, L. Huang, S. Liang, R. Liang, N. Qin, L. Wu, Electrostatically derived self-assembly of NH 2-mediated zirconium MOFs with graphene for photocatalytic reduction of Cr(vi), RSC Adv. 4 (2014) 2546–2549.
[131] E. Dhivya, D. Magadevan, Y. Palguna, T. Mishra, N. Aman, Synthesis of titanium based hetero MOF photocatalyst for reduction of Cr (VI) from wastewater, J. Environ.Chem.Eng. 7 (2019), 103240.
[132] H. Wang, X. Yuan, Y. Wu, X. Chen, L. Leng, G. Zeng, Photodeposition of metal sulfides on titanium metal–organic frameworks for excellent visible-light-driven photocatalytic Cr (VI) reduction, RSC Adv. 5 (2015) 32531–32535.
[133] H. Xie, D. Ma, W. Liu, Q. Chen, Y. Zhang, J. Huang, H. Zhang, Z. Jin, T. Luo, F. Peng, Zr-Based MOFs as new photocatalysts for the rapid reduction of Cr (vi) in water, New J. Chem. 44 (2020) 7218–7225.
[134] M.B. Hussain, U. Azhar, H.M. Loussala, R. Razaq, Synergetic effect of ZnIn2S4 nanosheets with metal-organic framework molding heterostructure for efficient visible-light driven photocatalytic reduction of Cr(VI), Arab. J. Chem. 13 (2020) 5939–5948.
[135] Z. Zhang, S. Wang, M. Bao, J. Ren, S. Pei, S. Yu, J. Ke, Construction of ternary Ag/AgCl/NH2-UiO-66 hybridized heterojunction for effective photocatalytic hexavalent chromium reduction, J. Colloid Interface Sci. 555 (2019) 342–351.
[136] R. Liang, F. Jing, L. Shen, N. Qin, L. Wu, MIL-53 (Fe) as a highly efficient bifunctional photocatalyst for the simultaneous reduction of Cr (VI) and oxidation of dyes, J. Hazard. Mater. 287 (2015) 364–372.
[137] Q. Xia, B. Huang, X. Yuan, H. Wang, Z. Wu, L. Jiang, T. Xiong, J. Zhang, G. Zeng, H. Wang, Modified stannous sulfide nanoparticles with metal-organic framework: toward efficient and enhanced photocatalytic reduction of chromium (VI) under visible light, J. Colloid Interface Sci. 530 (2018) 481–492.
[138] X. Du, X. Yi, P. Wang, J. Deng, C.-C. Wang, Enhanced photocatalytic Cr (VI) reduction and diclofenac sodium degradation under simulated sunlight irradiation over MIL-100 (Fe)/g-C3N4 heterojunctions, Chin. J. Catal. 40 (2019) 70–79.
[139] L. Shao, Z. Yu, X. Li, X. Li, H. Zeng, X. Feng, Carbon nanodots anchored onto the metal-organic framework NH2-MIL-88B (Fe) as a novel visible light-driven photocatalyst: photocatalytic performance and mechanism investigation, Appl. Surf. Sci. 505 (2020), 144616.
[140] R. Liang, L. Shen, F. Jing, W. Wu, N. Qin, R. Lin, L. Wu, NH2-mediated indium metal–organic framework as a novel visible-light-driven photocatalyst for reduction of the aqueous Cr(VI), Appl. Catal. B Environ. 162 (2015) 245–251.
[141] Y. Pi, X. Li, Q. Xia, J. Wu, Z. Li, Y. Li, J. Xiao, Formation of willow leaf-like structures composed of NH2-MIL68 (In) on a multifunctional multiwalled carbon nanotube backbone for enhanced photocatalytic reduction of Cr (VI), Nano Res. 10 (2017) 3543–3556.
[142] L. Wang, T. Zeng, G. Liao, Q. Cheng, Z. Pan, Syntheses, structures and catalytic mechanisms of three new MOFs for aqueous Cr (VI) reduction and dye degradation under UV light, Polyhedron 157 (2019) 152–162.
[143] H. Yang, L. Jiang, W. Wang, Z. Luo, J. Li, Z. He, Z. Yan, J. Wang, One-pot synthesis of CdS/metal–organic framework aerogel composites for efficient visible photocatalytic reduction of aqueous Cr(vi), RSC Adv. 9 (2019) 37594–37597.
[144] H. Kaur, S. Sinha, V. Krishnan, R.R. Koner, Photocatalytic reduction and recognition of Cr (VI): new Zn (II)-based metal–organic framework as catalytic surface, Ind. Eng. Chem. Res. 59 (2020) 8538–8550.
[145] C. Hu, Y.-C. Huang, A.-L. Chang, M. Nomura, Amine functionalized ZIF-8 as a visible-light-driven photocatalyst for Cr (VI) reduction, J. Colloid Interface Sci. 553 (2019) 372–381.
[146] X. Xu, S. Xiao, H.J. Willy, T. Xiong, R. Borayek, W. Chen, D. Zhang, J. Ding, 3D-printed grids with polymeric photocatalytic system as flexible air filter, Appl. Catal. B Environ. 262 (2020), 118307.
[147] L. Chen, Y. Honsho, S. Seki, D. Jiang, Light-harvesting conjugated microporous polymers: rapid and highly efficient flow of light energy with a porous polyphenylene framework as antenna, J. Am. Chem. Soc. 132 (2010) 6742–6748.
[148] Y.-L. Wong, J. Tobin, Z. Xu, F. Vilela, Conjugated porous polymers for photocatalytic applications, J. Mater. Chem. A 4 (2016) 18677–18686.
[149] Z. Ajma, Y. Naciri, R. Djellabi, N. Hassan, S. Zaman, A. Murtaza, A. Kumar, A. G. Al-Sehemi, H. Algarni, M. ul Haq, Recent advancement in conjugated polymers based photocatalytic technology for air pollutants abatement: cases of CO2, NOx, and VOCs, Chemosphere 136358 (2022).
[150] W.-Y. Geng, S.-F. Guo, H. Zhang, Y.-H. Luo, X.-X. Lu, F.-Y. Chen, Z.-X. Wang, D.-E. Zhang, Assembly of anthracene-based donor-acceptor conjugated organic polymers for efficient photocatalytic aqueous Cr (VI) reduction and organic pollution degradation under visible light, J. Solid State Chem. 310 (2022), 123004.
[151] R. Djellabi, X. Zhao, C.L. Bianchi, P. Su, J. Ali, B. Yang, Visible light responsive photoactive polymer supported on carbonaceous biomass for photocatalytic water remediation, J. Clean. Prod. 269 (2020), 122286.
[152] K. Wang, P. Chen, W. Nie, Y. Xu, Y. Zhou, Improved photocatalytic reduction of Cr (VI) by molybdenum disulfide modified with conjugated polyvinyl alcohol, Chem. Eng. J. 359 (2019) 1205–1214.
[153] D. Liu, Y. Wang, X. Xu, Y. Xiang, Z. Yang, P. Wang, Highly efficient photocatalytic Cr (VI) reduction by lead molybdate wrapped with DA conjugated polymer under visible light, Catalysts 11 (2021) 106.
[154] J. Wen, J. Xie, X. Chen, X. Li, A review on g-C3N4-based photocatalysts, Appl. Surf. Sci. 391 (2017) 72–123.
[155] J. Fu, J. Yu, C. Jiang, B. Cheng, g-C3N4-Based heterostructured photocatalysts, Adv. Energy Mater. 8 (2018), 1701503.
[156] Z. Li, Z.-J. Jiang, J.-F. Zheng, M.-J. Lin, Donor-acceptor conjugated heptazine polymers: boosting the Cr (VI) photoreductions via heteroatom engineering, <sb:contribution><sb:title>Mater. Today</sb:title></sb:contribution><sb:host><sb:issue><sb:series><sb:title>Commun.</sb:title></sb:series></sb:issue></sb:host> (2022), 103825.
[157] Y. Wang, W. Zhang, Y. Yang, J. Tang, C. Pan, Y.-N. Liu, R. Abu-Reziq, G. Yu, Visible-light-driven Cr (VI) reduction by ferrocene-integrated conjugated porous polymers via dual catalytic routes, Chem. Commun. 57 (2021) 4886–4889.
[158] F. Fu, W. Han, B. Tang, M. Hu, Z. Cheng, Insights into environmental remediation of heavy metal and organic pollutants: simultaneous removal of hexavalent chromium and dye from wastewater by zero-valent iron with ligand-enhanced reactivity, Chem. Eng. J. 232 (2013) 534–540.
[159] X. Hu, H. Ji, F. Chang, Y. Luo, Simultaneous photocatalytic Cr (VI) reduction and 2, 4, 6-TCP oxidation over g-C3N4 under visible light irradiation, Catal. Today 224 (2014) 34–40.
[160] Y. Zhang, Z. Chen, S. Liu, Y.-J. Xu, Size effect induced activity enhancement and anti-photocorrosion of reduced graphene oxide/ZnO composites for degradation of organic dyes and reduction of Cr (VI) in water, Appl. Catal. B Environ. 140 (2013) 598–607.
[161] R. Djellabi, M.F. Ghorab, T. Sehili, Simultaneous removal of methylene blue and hexavalent chromium from water using TiO2/Fe (III)/H2O2/sunlight, CLEAN–Soil,Air, Water 45 (2017) 1500379.
[162] S. Schrank, H. José, R. Moreira, Simultaneous photocatalytic Cr (VI) reduction and dye oxidation in a TiO2 slurry reactor, J. Photochem. Photobiol. A Chem. 147 (2002) 71–76.
[163] Q. Yuan, L. Chen, M. Xiong, J. He, S.-L. Luo, C.-T. Au, S.-F. Yin, Cu2O/BiVO4 heterostructures: synthesis and application in simultaneous photocatalytic oxidation of organic dyes and reduction of Cr (VI) under visible light, Chem. Eng. J. 255 (2014) 394–402.
[164] A.-D. Xie, M.-G. Hu, Y.-H. Luo, X.-G. Zhu, Z.-H. Wang, W.-Y. Geng, H. Zhang, D.-E. Zhang, H. Zhang, Synthesis of a stable iron (III)–organic framework for a visible light induced simultaneous photocatalytic reduction of Cr (VI) and the degradation of organic dyes in water, New J. Chem. 45 (2021) 13406–13414.

[165] E. Liu, Y. Du, X. Bai, J. Fan, X. Hu, Synergistic improvement of Cr (VI) reduction and RhB degradation using RP/g-C3N4 photocatalyst under visible light irradiation, Arab. J. Chem. 13 (2020) 3836–3848.
[166] U. Alam, A. Khan, D. Bahnemann, M. Muneer, Synthesis of Co doped ZnWO4 for simultaneous oxidation of RhB and reduction of Cr (VI) under UV-light irradiation, J.Environ.Chem.Eng. 6 (2018) 4885–4898.
[167] H. Liu, T. Liu, Z. Zhang, X. Dong, Y. Liu, Z. Zhu, Simultaneous conversion of organic dye and Cr (VI) by SnO2/rGO microcomposites, J. Mol. Catal. A Chem. 410 (2015) 41–48.
[168] H. Yu, S. Chen, X. Quan, H. Zhao, Y. Zhang, Fabrication of a TiO2− BDD heterojunction and its application as a photocatalyst for the simultaneous oxidation of an azo dye and reduction of Cr(VI), Environ.Sci.Technol. 42 (2008) 3791–3796.
[169] Q. Zhang, Y. Han, L. Wu, Influence of electrostatic field on the adsorption of phenol on single-walled carbon nanotubes: a study by molecular dynamics simulation, Chem. Eng. J. 363 (2019) 278–284.
[170] K. Wang, X. Liu, J. Tang, L. Wang, H. Sun, Ball milled Fe0@ FeS hybrids coupled with peroxydisulfate for Cr (VI) and phenol removal: novel surface reduction and activation mechanisms, Sci. Total Environ. 739 (2020), 139748.
[171] B.S. Rathi, P.S. Kumar, P.-L. Show, A review on effective removal of emerging contaminants from aquatic systems: current trends and scope for further research, J. Hazard. Mater. 409 (2021), 124413.
[172] R. Mu, Z. Xu, L. Li, Y. Shao, H. Wan, S. Zheng, On the photocatalytic properties of elongated TiO2 nanoparticles for phenol degradation and Cr (VI) reduction, J. Hazard. Mater. 176 (2010) 495–502.
[173] L. Huang, Q. Chan, X. Wu, H. Wang, Y. Liu, The simultaneous photocatalytic degradation of phenol and reduction of Cr (VI) by TiO2/CNTs, J. Ind. Eng. Chem. 18 (2012) 574–580.
[174] D. Lu, W. Chai, M. Yang, P. Fang, W. Wu, B. Zhao, R. Xiong, H. Wang, Visible light induced photocatalytic removal of Cr (VI) over TiO2-based nanosheets loaded with surface-enriched CoOx nanoparticles and its synergism with phenol oxidation, Appl. Catal. B Environ. 190 (2016) 44–65.
[175] T. Yu, L. Lv, H. Wang, X. Tan, Enhanced photocatalytic treatment of Cr (VI) and phenol by monoclinic BiVO4 with {010}-orientation growth, Mater. Res. Bull. 107 (2018) 248–254.
[176] D.K. Padhi, T.K. Panigrahi, K. Parida, S. Singh, P. Mishra, Green synthesis of Fe3O4/RGO nanocomposite with enhanced photocatalytic performance for Cr (VI) reduction, phenol degradation, and antibacterial activity, ACS Sustain. Chem. Eng. 5 (2017) 10551–10562.
[177] H. Ma, J. Shen, M. Shi, X. Lu, Z. Li, Y. Long, N. Li, M. Ye, Significant enhanced performance for Rhodamine B, phenol and Cr (VI) removal by Bi2WO6 nancomposites via reduced graphene oxide modification, Appl. Catal. B Environ. 121 (2012) 198–205.
[178] Z. Jin, Y.-X. Zhang, F.-L. Meng, Y. Jia, T. Luo, X.-Y. Yu, J. Wang, J.-H. Liu, X.-J. Huang, Facile synthesis of porous single crystalline ZnO nanoplates and their application in photocatalytic reduction of Cr (VI) in the presence of phenol, J. Hazard. Mater. 276 (2014) 400–407.
[179] S. Patnaik, K.K. Das, A. Mohanty, K. Parida, Enhanced photo catalytic reduction of Cr(VI) over polymer-sensitized g-C3N4/ZnFe2O4 and its synergism with phenol oxidation under visible light irradiation, Catal. Today 315 (2018) 52–66.
[180] S. Nayak, K. Parida, Dynamics of charge-transfer behavior in a plasmon-induced quasi-type-II p–n/n–n dual heterojunction in Ag@ Ag3PO4/g-C3N4/NiFe LDH nanocomposites for photocatalytic Cr (VI) reduction and phenol oxidation, ACS Omega 3 (2018) 7324–7343.
[181] Y.-X. Li, X. Wang, C.-C. Wang, H. Fu, Y. Liu, P. Wang, C. Zhao, S-TiO2/UiO-66-NH2 composite for boosted photocatalytic Cr (VI) reduction and bisphenol A degradation under LED visible light, J. Hazard. Mater. 399 (2020), 123085.
[182] J.-W. Wang, F.-G. Qiu, P. Wang, C. Ge, C.-C. Wang, Boosted bisphenol A and Cr (VI) cleanup over Z-scheme WO3/MIL-100 (Fe) composites under visible light, J. Clean. Prod. 279 (2021), 123408.
[183] J. Gong, W. Zhang, T. Sen, Y. Yu, Y. Liu, J. Zhang, L. Wang, Metal-Organic Framework MIL-101 (Fe) nanoparticles decorated with Ag nanoparticles for regulating the photocatalytic phenol oxidation pathway for Cr (VI) reduction, ACS Appl.Nano Mater. 4 (2021) 4513–4521.
[184] S. Zhang, H. Lan, Y. Cui, X. An, H. Liu, J. Qu, Insight into the key role of Cr intermediates in the efficient and simultaneous degradation of organic contaminants and Cr (VI) reduction via g-C3N4-assisted photocatalysis, Environ. Sci.Technol. 56 (2022) 3552–3563.
[185] M. Carballa, F. Omil, T. Ternes, J.M. Lema, Fate of pharmaceutical and personal care products (PPCPs) during anaerobic digestion of sewage sludge, Water Res. 41 (2007) 2139–2150.
[186] S. Suarez, J.M. Lema, F. Omil, Removal of pharmaceutical and personal care products (PPCPs) under nitrifying and denitrifying conditions, Water Res. 44 (2010) 3214–3224.
[187] J.W. O'Brien, A.P.W. Banks, A.J. Novic, J.F. Mueller, G. Jiang, C. Ort, G. Eaglesham, Z. Yuan, P.K. Thai, Impact of in-sewer degradation of pharmaceutical and personal care products (PPCPs) population markers on a population model, Environ.Sci.Technol. 51 (2017) 3816–3823.
[188] X. Yang, R.C. Flowers, H.S. Weinberg, P.C. Singer, Occurrence and removal of pharmaceuticals and personal care products (PPCPs) in an advanced wastewater reclamation plant, Water Res. 45 (2011) 5218–5228.
[189] D.-D. Chen, X.-H. Yi, C. Zhao, H. Fu, P. Wang, C.-C. Wang, Polyaniline modified MIL-100 (Fe) for enhanced photocatalytic Cr (VI) reduction and tetracycline degradation under white light, Chemosphere 245 (2020), 125659.
[190] F. Liu, Z. Ma, Y. Deng, M. Wang, P. Zhou, W. Liu, S. Guo, M. Tong, D. Ma, Tunable covalent organic frameworks with different heterocyclic nitrogen locations for efficient Cr (VI) reduction, Escherichia coli disinfection, and paracetamol degradation under visible-light irradiation, Environ. Sci. Technol. 55 (2021) 5371–5381.
[191] N. Wang, W.L. Budde, Determination of carbamate, urea, and thiourea pesticides and herbicides in water, Anal. Chem. 73 (2001) 997–1006.
[192] M. Cerejeira, P. Viana, S. Batista, T. Pereira, E. Silva, M. Valério, A. Silva, M. Ferreira, A. Silva-Fernandes, Pesticides in Portuguese surface and ground waters, Water Res. 37 (2003) 1055–1063.
[193] Y. Li, P. Su, Y. Li, K. Wen, G. Bi, M. Cox, Adsorption-desorption and degradation of insecticides clothianidin and thiamethoxam in agricultural soils, Chemosphere 207 (2018) 708–714.
[194] L. Yang, W. Sun, S. Luo, Y. Luo, White fungus-like mesoporous Bi2S3 ball/TiO2 heterojunction with high photocatalytic efficiency in purifying 2, 4-dichloro-phenoxyacetic acid/Cr (VI) contaminated water, Appl. Catal. B Environ. 156 (2014) 25–34.
[195] A.A. Oladipo, MIL-53 (Fe)-based photo-sensitive composite for degradation of organochlorinated herbicide and enhanced reduction of Cr (VI), Process. Saf. Environ. Prot. 116 (2018) 413–423.
[196] D. Majhi, A.K. Mishra, K. Das, R. Bariki, B. Mishra, Plasmonic Ag nanoparticle decorated Bi2O3/CuBi2O4 photocatalyst for expeditious degradation of 17α-ethinylestradiol and Cr (VI) reduction: insight into electron transfer mechanism and enhanced photocatalytic activity, Chem. Eng. J. 413 (2021), 127506.
[197] Q. Sun, B. Han, K. Li, L. Yu, L. Dong, The synergetic degradation of organic pollutants and removal of Cr (VI) in a multifunctional dual-chamber photocatalytic fuel cell with Ag@ Fe2O3 cathode, Sep. Purif. Technol. 281 (2022), 119966.
[198] H. Liang, T. Li, J. Zhang, D. Zhou, C. Hu, X. An, R. Liu, H. Liu, 3-D hierarchical Ag/ZnO@ CF for synergistically removing phenol and Cr (VI): heterogeneous vs. homogeneous photocatalysis, J. Colloid Interface Sci. 558 (2020) 85–94.
[199] F. Yang, Y. Guo, C. Li, D. Tang, H. Jiang, G. Wang, K. Xuan, Facile fabrication of AgFe1− xCuxO2 composite with abundant oxygen vacancies for boosted photocatalytic Cr (VI) reduction and organic pollutants degradation under visible light, Colloids Surf. A Physicochem. Eng. Asp. 628 (2021), 127305.
[200] Y. Zhang, Z. Chen, Z. Shi, T.-T. Lu, D. Chen, Q. Wang, Z. Zhan, A direct Z-scheme BiOBr/TzDa COF heterojunction photocatalyst with enhanced performance on visible-light driven removal of organic dye and Cr (VI), Sep. Purif. Technol. 275 (2021), 119216.
[201] G. Zhao, Y. Sun, Y. Zhao, T. Wen, X. Wang, Z. Chen, G. Sheng, C. Chen, X. Wang, Enhanced photocatalytic simultaneous removals of Cr (VI) and bisphenol A over Co (II)-modified TiO2, Langmuir 35 (2018) 276–283.
[202] Y. Yang, G. Wang, Q. Deng, D.H. Ng, H. Zhao, Microwave-assisted fabrication of nanoparticulate TiO2 microspheres for synergistic photocatalytic removal of Cr (VI) and methyl orange, ACS Appl. Mater. Interfaces 6 (2014) 3008–3015.
[203] H. Guo, C.-G. Niu, L. Zhang, X.-J. Wen, C. Liang, X.-G. Zhang, D.-L. Guan, N. Tang, G.-M. Zeng, Construction of direct Z-scheme AgI/Bi2Sn2O7 nanojunction system with enhanced photocatalytic activity: accelerated interfacial charge transfer induced efficient Cr (VI) reduction, tetracycline degradation and Escherichia coli inactivation, ACS Sustain. Chem. Eng. 6 (2018) 8003–8018.
[204] Z. He, L. Jiang, D. Wang, J. Qiu, J. Chen, S. Song, Simultaneous oxidation of p-chlorophenol and reduction of Cr (VI) on fluorinated anatase TiO2 nanosheets with dominant {001} facets under visible irradiation, Ind. Eng. Chem. Res. 54 (2015) 808–818.
[205] Q. Zhang, Y. Fu, Y. Wu, Y.-N. Zhang, T. Zuo, Low-cost Y-doped TiO2 nanosheets film with highly reactive 001 facets from CRT waste and enhanced photocatalytic removal of Cr (VI) and methyl orange, ACS Sustain. Chem. Eng. 4 (2016) 1794–1803.
[206] L. Guo, J. Yang, H. Zhang, R. Wang, J. Xu, J. Wang, Highly enhanced visible-light photocatalytic activity via a novel surface structure of CeO2/g− C3N4 toward removal of 2, 4-dichlorophenol and Cr (VI), ChemCatChem 13 (2021) 2034–2044.
[207] J. Li, C. Xiao, K. Wang, Y. Li, G. Zhang, Enhanced generation of reactive oxygen species under visible light irradiation by adjusting the exposed facet of FeWO4 nanosheets to activate oxalic acid for organic pollutant removal and Cr (VI) reduction, Environ.Sci.Technol. 53 (2019) 11023–11030.
[208] J.-C. Wang, J. Ren, H.-C. Yao, L. Zhang, J.-S. Wang, S.-Q. Zang, L.-F. Han, Z.-J. Li, Synergistic photocatalysis of Cr (VI) reduction and 4-Chlorophenol degradation over hydroxylated α-Fe2O3 under visible light irradiation, J. Hazard. Mater. 311 (2016) 11–19.
[209] A. Giannakas, M. Antonopoulou, C. Daikopoulos, Y. Deligiannakis, I. Konstantinou, Characterization and catalytic performance of B-doped, B-N co-doped and B–N–F tri-doped TiO2 towards simultaneous Cr (VI) reduction and benzoic acid oxidation, Appl. Catal. B Environ. 184 (2016) 44–54.
[210] S.K. Loeb, P.J. Alvarez, J.A. Brame, E.L. Cates, W. Choi, J. Crittenden, D. D. Dionysiou, Q. Li, G. Li-Puma, X. Quan, The Technology Horizon for Photocatalytic Water Treatment: Sunrise or Sunset? ACS Publications, 2018.
[211] B.A. Marinho, R.O. Cristovao, J.M. Loureiro, R.A. Boaventura, V.J. Vilar, Solar photocatalytic reduction of Cr (VI) over Fe (III) in the presence of organic sacrificial agents, Appl. Catal. B Environ. 192 (2016) 208–219.
[212] H. Arslan, O. Eskikaya, Z. Bilici, N. Dizge, D. Balakrishnan, Comparison of Cr (VI) adsorption and photocatalytic reduction efficiency using leonardite powder, Chemosphere 300 (2022), 134492.
[213] F. Fu, Q. Wang, Removal of heavy metal ions from wastewaters: a review, J. Environ. Manag. 92 (2011) 407–418.
[214] J. Bratby, Coagulation and Flocculation in Water and Wastewater Treatment, IWA Publishing, 2016.

[215] H.Y. Shim, K.S. Lee, D.S. Lee, D.S. Jeon, M.S. Park, J.S. Shin, Y.K. Lee, J.W. Goo, S.B. Kim, D.Y. Chung, Application of electrocoagulation and electrolysis on the precipitation of heavy metals and particulate solids in washwater from the soil washing, J.Agric.Chem.Environ. 3 (2014) 130.

[216] S.M. Doke, G.D. Yadav, Process efficacy and novelty of titania membrane prepared by polymeric sol–gel method in removal of chromium (VI) by surfactant enhanced microfiltration, Chem. Eng. J. 255 (2014) 483–491.

[217] L. Feng, K.-Y. Wang, G.S. Day, M.R. Ryder, H.-C. Zhou, Destruction of metal–organic frameworks: positive and negative aspects of stability and lability, Chem. Rev. 120 (2020) 13087–13133.